RSC Advances

PAPER

View Article Online
View Journal | View Issue

Cite this: *RSC Adv.*, 2026, **16**, 11137

Eco-conscious and cost-effective electrochemical sensor for selective determination of eszopiclone in pure form, alkaline-stressed samples, and pharmaceutical tablets

Feda A. H. Elgammal, Marwa S. Moneeb, Suzy M. Sabry and Amira F. El-Yazbi *

A novel, rapid, economic, and environmentally friendly voltammetric method using a pretreated pencil graphite electrode (PPGE) was employed for eszopiclone (EZP) determination in its pure form, tablet formulation, and in the presence of its alkaline degradants using differential pulse (DPV) and square wave (SWV) techniques. The impact of both potentiostatic and potentiodynamic pretreatment strategies on the electrode analytical performance was investigated. The PPGE exhibited superior electrocatalytic activity compared to the non-pretreated pencil graphite electrode (NPGE) and the glassy carbon electrode (GCE). Moreover, the influence of surfactant addition on the peak current was studied. The use of sodium dodecyl sulfate (SDS) surfactant enhanced the concentration range of measurements to 2.5–300 μg mL^{-1} with a limit of quantitation (LOQ) of 2.443 μg mL^{-1} and a limit of detection (LOD) of 0.733 μg mL^{-1}. A further sensitivity enhancement was achieved using the differential pulse adsorptive stripping voltammetric (DP-AdSV) technique, extending the linear concentration range to 0.25–15 μg mL^{-1} with a LOQ of 0.195 μg mL^{-1} and a LOD of 0.058 μg mL^{-1}. The PPGE was successfully characterized using scanning electron microscopy, X-ray diffraction, and Fourier transform infrared. The method was rigorously validated as per ICH guidelines and its environmental sustainability was quantitatively assessed using the Analytical Eco-Scale and the Green Analytical Procedure Index (GAPI). Furthermore, the method's overall "whiteness" was assessed using the recently released Red-Green-Blue (RGB) 12 model approach, reflecting the balance between analytical performance, environmental impact, and practical applicability.

Received 10th January 2026
Accepted 14th February 2026

DOI: 10.1039/d6ra00252h

rsc.li/rsc-advances

1. Introduction

Eszopiclone (EZP), the active *S* enantiomer of zopiclone (ZP), is a cyclopyrrolone-class hypnotic agent with the chemical name (+)-(5*S*)-6-(5-chloropyridin-2-yl)-7-oxo-6, 7-dihydro-5*H*-pyrrolo [3,4-*b*] pyrazin-5-yl-4-methylpiperazine-1-carboxylate and a molecular formula of $C_{17}H_{17}ClN_6O_3$ with a molecular weight of 388.81 g mol^{-1} (Fig. 1).[1,2]

Various analytical methods have been reported for EZP quantification, including UV spectrophotometry,[3–6] spectrofluorometry,[7] high-performance liquid chromatography (HPLC),[8–12] ultra-performance liquid chromatography (UPLC),[13,14] gas chromatography (GC),[11] high-performance thin-layer chromatography (HPTLC)[7,15,16] and capillary electrophoresis (CE).[17] However, these techniques often require costly instrumentation and trained personnel, and involve significant consumption of hazardous solvents.[18] Electrochemical analysis provides an attractive alternative due to its simplicity, sensitivity, rapidity, affordability, and suitability for on-site applications.[19–22] The first electrochemical assay for EZP was a potentiometric method reported by our group.[23] Later, a voltammetric GCE method demonstrated linearity from 3×10^{-6} to 5×10^{-5} M with LOQ and LOD of 6.41×10^{-8} M and 1.9×10^{-8} M, respectively.[24]

In electrochemical analysis, methods based on achiral electrodes, such as PGE, in the absence of specific chiral recognition elements generally do not provide stereoselective responses. As stereoisomers exhibit identical physicochemical

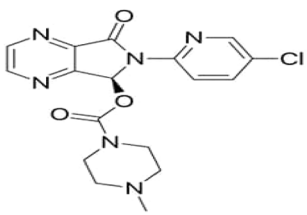

Fig. 1 Chemical structure of EZP.

Faculty of Pharmacy, Department of Pharmaceutical Analytical Chemistry, University of Alexandria, El-Messalah, Alexandria 21521, Egypt. E-mail: amira.elyazbi@alexu.edu.eg

and redox properties in achiral environments, both stereoisomers are expected to display similar electrochemical behavior under the applied experimental conditions.[23,25] On this basis, it is important to reference previously reported voltammetric methods for the racemic ZP determination. Voltammetric and adsorptive stripping voltammetric (AdSV) methods have been published for ZP, addressing oxidation and reduction behavior using GCE and DME electrodes.[26–28]

PGEs represent a green, low-cost alternative to conventional electrodes. They offer excellent conductivity, mechanical stability, disposability, and simple surface renewal by mechanical extrusion.[29–36] Their performance can be further enhanced through electrochemical pretreatment or surface modification strategies.[37–44] Electrochemical pretreatment is particularly attractive as it is rapid, inexpensive, and requires no hazardous reagents.[45] This pretreatment can be performed using either potentiostatic or potentiodynamic strategies. In the potentiostatic approach, the electrode is maintained at a selected potential in an electrolyte solution for a certain time. In contrast, the potentiodynamic pretreatment involves scanning the potential for a specific number of cycles at a certain scan rate.[37,46]

The present work introduces the first voltammetric method for EZP determination using an electrochemically pretreated pencil graphite electrode (PPGE). To validate the structural and surface properties of the PPGE, it was thoroughly characterized using SEM, XRD, and FT-IR. This method enables quantification of EZP in pure form, tablet dosage forms, and in the presence of alkaline degradants. It also investigates the effects of surfactants, applies stripping voltammetry to enhance sensitivity,[47] and compares PPGE performance with bare PGE and GCE. Practical relevance is emphasized through its simplicity, cost-effectiveness, and alignment with green analytical chemistry (GAC) and white analytical chemistry (WAC) principles.[46] Greenness and whiteness were evaluated using the Analytical Eco-Scale, GAPI, and the RGB 12-model. Finally, the results obtained were compared with those from a reported HPLC method to assess the accuracy and reliability of the proposed method. To our knowledge, neither PGE nor PPGE has previously been employed for EZP analysis, marking this as the first such application.

2. Experimental

2.1. Equipment

The instrument used for the polarographic measurements was a computer-controlled VA Computrace voltammetric analyzer, model 797, equipped with a multimode electrode (MME) (Metrohm, Herisau, Switzerland). The electrolytic cell consisted of a PPGE as a working electrode, an Ag/AgCl reference electrode filled with 3 M KCl solution, and a platinum auxiliary electrode. pH measurements were carried out using a Cyberscan (510) pH meter (Thermo Orion Beverly, MA, USA).

Hi-polymer graphite pencil HB black leads (60 mm length and 0.9 mm diameter) were obtained from Rotring, Germany. For electrical connection, a copper wire was attached to 15 mm segment of the lead extending from a Rotring mechanical pencil. The pencil was held vertically with a 10 mm length of the lead immersed in the solution.

The electrode characterization was achieved using L-1600400 spectrum two FT-IR spectrometer equipped with deuterated triglycine sulfate (DTGS) detector (PerkinElmer, United Kingdom), and LabX XRD-6100 X-ray diffractometer with Cu Kα radiation of $\lambda = 1.540598$ Å (Shimadzu, Japan). Electrode surface imaging was performed using JSM-6360 LA scanning electron microscope (Jeol, Japan).

2.2. Reagents and chemicals

An authentic sample of EZP was kindly provided by Medizen Pharmaceuticals, Alexandria, Egypt. The pharmaceutical dosage form, *Night Calm®* tablets containing 3 mg of EZP per tablet (Medizen Pharmaceuticals, Egypt), was procured from a local pharmacy. *O*-Phosphoric acid was obtained from LOBA Chemie PVT-LTD, Mumbai, India. Sodium hydroxide, sodium chloride, boric acid, and glacial acetic acid, in addition to surfactants sodium dodecyl sulfate (SDS), tween 80, and cetyltrimethylammonium bromide (CTAB), were bought from El-Nasr Chemical Industry Company, Egypt. Lactose, glucose, starch and the chloride salts of calcium, potassium, and sodium were employed as potential interfering agents and were obtained from El Nasr Pharmaceutical Chemicals, Egypt. Deionized water was utilized throughout all experiments. All the reagents and chemicals were of analytical grade and were utilized as supplied, without further purification.

2.3. Electrochemical pretreatment and instrumental measurement parameters

To activate the PGE surface and enhance its electrochemical performance, a pretreatment step was carried out before the voltammetric analysis and quantification of EZP. Before DPV measurements, a potentiodynamic pretreatment was performed by applying cyclic voltammetry (CV) and scanning the electrode over a potential range of 0 to 2 V at a scan rate of 50 mV s^{-1} for 100 scan cycles in 0.04 M Britton–Robinson (BR) buffer/0.1 M NaCl solution, pH 7. Before SWV measurements, a potentiostatic pretreatment was performed by applying CV at a constant potential of −1.5 V for 180 s in the same pretreatment solution.

After pretreatment, the PPGEs were washed twice by gentle dipping in deionized water, followed by DPV and SWV measurements of EZP. The optimal parameters for DPV measurements were as follows: pulse time = 0.04 s, pulse amplitude = 50 mV, and potential sweep rate = 80 mV s^{-1}. For SWV measurement, the optimized parameters were frequency = 50 Hz, pulse step = 10 mV, and pulse amplitude = 40 mV.

2.4. Preparation of stock and working standard solutions

A stock solution of 1000 μg per mL EZP was prepared by dissolving 50 mg of drug in 50 mL 0.01 M BR buffer, pH 3.2. The stock solution was kept in the refrigerator and freshly prepared daily. The stock solution was appropriately diluted using 0.01 M BR buffer/0.1 M NaCl solution, pH 7, to prepare working standard solutions covering the desired linear concentration range.

Table 1 Regression data of the calibration lines of EZP using DPV, SWV, and AdSV techniques

Parameters / Techniques	SWV (in 0.01 M BR buffer/0.1 M NaCl solution, pH 7)	DPV (in 0.01 M BR buffer/0.1 M NaCl solution, pH 7)	DPV (in 0.01 M BR buffer/0.004 M SDS solution, pH 7)	AdSV (in 0.01 M BR buffer/0.1 M NaCl solution, pH 7)
Measured potential (V)	1.1902	1.1009	1.1009	1.1009
Linear concentration range (μg mL^{-1})	15–400	10–500	2.5–300	0.25–15
Slope (*a*)	0.602	0.388	1.147	24.323
RSD of slope	0.004	0.002	0.007	0.115
Intercept (*b*)	1.678	2.902	7.983	1.475
RSD of intercept	0.778	0.381	0.872	0.825
Correlation coefficient (*r*)	0.9999	0.9999	0.9999	0.9999
Detection limit (μg mL^{-1})	2.219	2.114	0.733	0.058
Quantitation limit (μg mL^{-1})	7.395	7.047	2.443	0.195

2.5. Construction of calibration plots for DPV and SWV measurements

Precisely measured aliquots of EZP stock solution, within the concentration range indicated in Table 1, were transferred into a series of 10 mL volumetric flasks. Each flask was completed to the mark with 0.01 M BR buffer/0.1 M NaCl solution, pH 7. Before each measurement, the PPGE was rinsed with deionized water and gently wiped with a soft tissue to ensure a clean and reproducible surface. Using the optimized measurement parameters, DP- and SW-voltammograms were recorded over the potential range of 0 to +2 V *versus* Ag/AgCl reference electrode. The resulting peak currents were plotted against the corresponding EZP concentrations to construct the calibration curves.

2.6. Analysis of laboratory-prepared mixtures containing EZP with its alkaline degradation products

To evaluate the selectivity of the proposed method, a complete degradation of 300 μg per mL EZP was carried out using 2 M NaOH at 90 °C for 60 minutes.[48] After the specified degradation period, the solution was neutralized using 2 M HCl. The resulting solution was equivalent to 300 μg mL^{-1} of degradants. The complete EZP degradation was checked by HPLC on a Thermo Hypersil BDS 5 μ C18 column, 50 mm × 4.6 mm. The mobile phase is composed of methanol and 0.01 M phosphate of pH 2.5, adjusted with orthophosphoric acid in the ratio of 40 : 60 at a 1 mL min^{-1} flow rate. The detection was carried out at 304 nm.[48]

Mixtures composed of 300 μg mL^{-1} of EZP and varying concentrations of its alkaline degradant products (ranging from 1% to 70%) were prepared in 0.01 M BR buffer/0.1 M NaCl solution, pH 7. DPV measurements were carried out under optimized conditions. For each mixture, the peak current and peak potential were recorded. The percentage recovery was calculated by comparing the peak current readings with those of the standard 300 μg per mL EZP solution to detect any interference from its degradants.

2.7. Preparation of EZP tablet solutions

Twenty *Night Calm®* tablets were accurately weighed and finely ground into a uniform powder. A carefully weighted portion of the powdered tablets—equivalent to 50 mg of EZP—was extracted into 20 mL of 0.01 M BR buffer, pH 3.2, through 30 minutes of sonication in an ultrasonic bath followed by 2 minutes of centrifugation. The resulting supernatant was filtered into a 50 mL volumetric flask. The remaining residue was rinsed twice with 5 mL portions of the same BR buffer. The washing solutions were mixed with the filtrate, and the volume was completed to 50 mL using the BR buffer. This stock solution had a final EZP concentration of 1000 μg mL^{-1}. Before voltammetric measurements, appropriate dilutions were made using 0.01 M BR buffer/0.1 M NaCl solution, pH 7.

3. Results and discussion

3.1. Development and optimization of PGE pretreatment strategies

The impact of the electrochemical surface pretreatment of the PGE on its electrocatalytic properties and performance toward EZP oxidation was investigated using two pretreatment strategies: potentiostatic and potentiodynamic. To evaluate the influence of these pretreatments, the electrochemical responses were recorded using DPV and SWV, employing the measurement parameters listed in Experimental section 2.3. The results obtained using PPGE were compared to those obtained using NPGE to conclude the optimal pretreatment strategy for better electroanalytical sensitivity.

In addition to the pretreatment strategy, the influence of the pretreatment solution on the EZP oxidation signal was assessed with respect to both the pH and the type of buffer used. Potentiostatic pretreatment strategy (−1.5 V potential for 180 s) and potentiodynamic pretreatment strategy (0 to 2 V scanning potential range, 100 scan cycles, and 50 mV per s scan rate) were conducted in the different pretreatment solutions under investigation. Electrochemical responses were then recorded using both DPV and SWV techniques.

To assess the effect of pH, pretreatments were conducted in 0.04 M BR buffer/0.1 M NaCl solution at pH values of 3, 7, and 12, adjusted by HCl or NaOH. The solution of pH 7 showed the highest EZP signal in both DPV and SWV measurements, along with the lowest background current. The EZP response at pH 3 was moderate, while pH 12 resulted in the lowest EZP signal and

the highest blank current. Therefore, pH 7 was selected for subsequent analysis.

The effect of buffer type was then examined using 0.04 M solutions of BR, acetate, and phosphate, each containing 0.1 M NaCl, at the optimized pH 7. After blank correction, the obtained results showed that the buffer type has no effect on both DPV and SWV EZP signals. However, differences were observed in the background signals: the SWV blank signal was slightly elevated in the phosphate buffer, while both DPV and SWV blank signals were extensively higher in the acetate buffer. These elevated background currents could interfere with analytical sensitivity and signal clarity. Based on the results, the pretreatment solution composed of 0.04 M BR buffer/0.1 M NaCl solution, pH 7, was chosen as the optimal pretreatment solution for subsequent experiments.

3.1.1. Optimization of potentiostatic pretreatment instrumental parameters

3.1.1.1. The pretreatment potential. Since the electrochemical pretreatment could be achieved either at positive or negative potentials,[49] the potentiostatic pretreatment study was conducted by applying CV at different potentials over a broad range on the negative and positive sides from −1.5 V to 2 V for 300 s in 0.04 M BR buffer/0.1 M NaCl solution, pH 7. The results showed that as the pretreatment potential shifted toward more positive values, the background signal was noticeably increased in both DPV and SWV measurements. However, EZP signal, after blank subtraction, remained nearly constant. Among all tested potentials, −1.5 V showed the highest DPV and SWV EZP response with the lowest background signal. Notably, no signs of electrode damage were observed throughout the entire potential range tested, indicating the stability of the electrode under these conditions. Based on these findings, a pretreatment potential of −1.5 V was identified as optimal, offering the best balance between signal enhancement and background minimization.

3.1.1.2. The pretreatment duration. The effect of PGE pretreatment duration on the EZP oxidation signal was studied using DPV and SWV measurements. Potentiostatic pretreatment was performed by applying CV at −1.5 V in 0.04 M BR buffer/0.1 M NaCl solution, pH 7, with durations ranging from 30 s to 300 s. The results showed that the EZP response increased with longer pretreatment times reaching maximum at 180 s. Beyond this point, the signal started to slightly decrease. The background signal remained constant throughout all tested pretreatment durations. Accordingly, 180 s was selected as the optimal pretreatment time (Fig. S1, SI File).

3.1.2. Optimization of potentiodynamic pretreatment instrumental parameters

3.1.2.1. The pretreatment potential range. To determine the optimal potential range for potentiodynamic pretreatment, CV scans were conducted under two conditions: varying the starting potential from −1.5 V to 1.5 V while fixing the end potential at 2 V, fixing the starting potential at −2 V while varying the end potential from −1.5 V to 1.5 V. All scans were carried out at a 50 mV per s scan rate for 100 cycles. Among the tested conditions, the pretreatment potential range of 0 to 2 V showed the maximum DPV EZP response with the lowest blank signal. Accordingly, the potential range of 0 to 2 V was selected as the

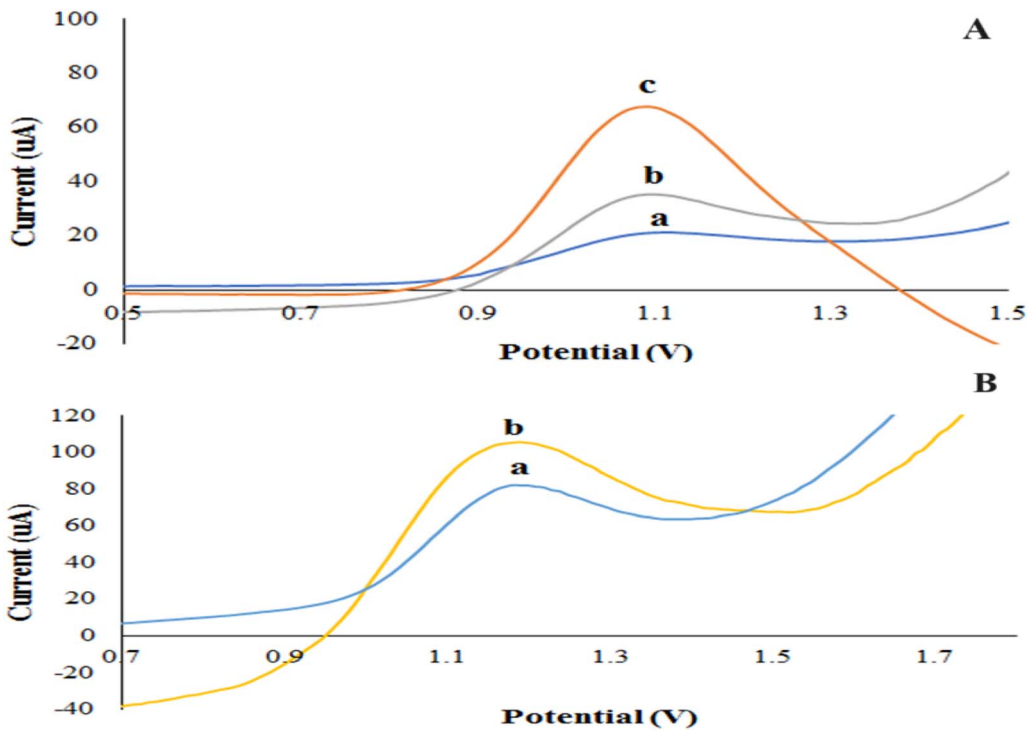

Fig. 2 Voltammograms of 300 μg per mL EZP prepared in 0.04 M BR buffer, pH 7 obtained by (a) non-pretreated PGE, (b) potentiostatically pretreated PGE, and (c) potentiodynamically pretreated PGE using (A) DPV at 1.1009 V and (B) SWV at 1.1902 V.

optimal window for potentiodynamic pretreatment in subsequent DPV measurements (Fig. S2, SI File).

It is important to note that all SWV measurements following potentiodynamic pretreatment across the tested potential ranges exhibited significantly elevated background signals. Therefore, the potentiodynamic pretreatment study was limited to DPV measurements.

3.1.2.2. The number of scan cycles. The influence of the scan count on the PPGE performance was investigated using a potential range of 0 to 2 V and a scan rate of 50 mV s^{-1} in 0.04 M BR buffer/0.1 M NaCl solution, pH 7. The results showed that as the number of scan cycles increased, the blank signal decreased, resulting in an enhancement in the EZP oxidation signal. The maximum DPV EZP response with minimal background interference was observed at 100 scan cycles (Fig. S3, SI File).

3.1.2.3. The influence of scan rate. The influence of scan rate on PPGE performance was studied at the optimized pretreatment conditions. The results showed that varying the scan rate had no effect on either the EZP signal or the blank signal.

3.2. Comparing the potentiodynamic and potentiostatic pretreatment strategies

After optimizing the parameters of both potentiodynamic and potentiostatic pretreatment strategies and comparing the resulting EZP peak currents obtained in the subsequent DPV measurements, it was found that potentiodynamically pretreated PGE provided a higher EZP response than that of potentiostatically pretreated PGE (Fig. 2A). Specifically, the potentiodynamic strategy enhanced the EZP oxidation peak current by a factor of 3.19, while the potentiostatic strategy resulted in an enhancement of EZP oxidation peak current by a factor of 1.67. Therefore, the potentiodynamic pretreatment strategy performed at a 0 to 2 V scanning potential range, 100 scan cycles, and a 50 mV per s scan rate in 0.04 M BR buffer/0.1 M NaCl solution, pH 7, was selected as the appropriate pretreatment approach for PGE activation before DPV measurements.

In contrast, during SWV measurements, the blank signals recorded with potentiodynamically pretreated PGE were dramatically high. As a result, the potentiostatic pretreatment strategy at −1.5 V potential for 180 s in 0.04 M BR buffer/0.1 M

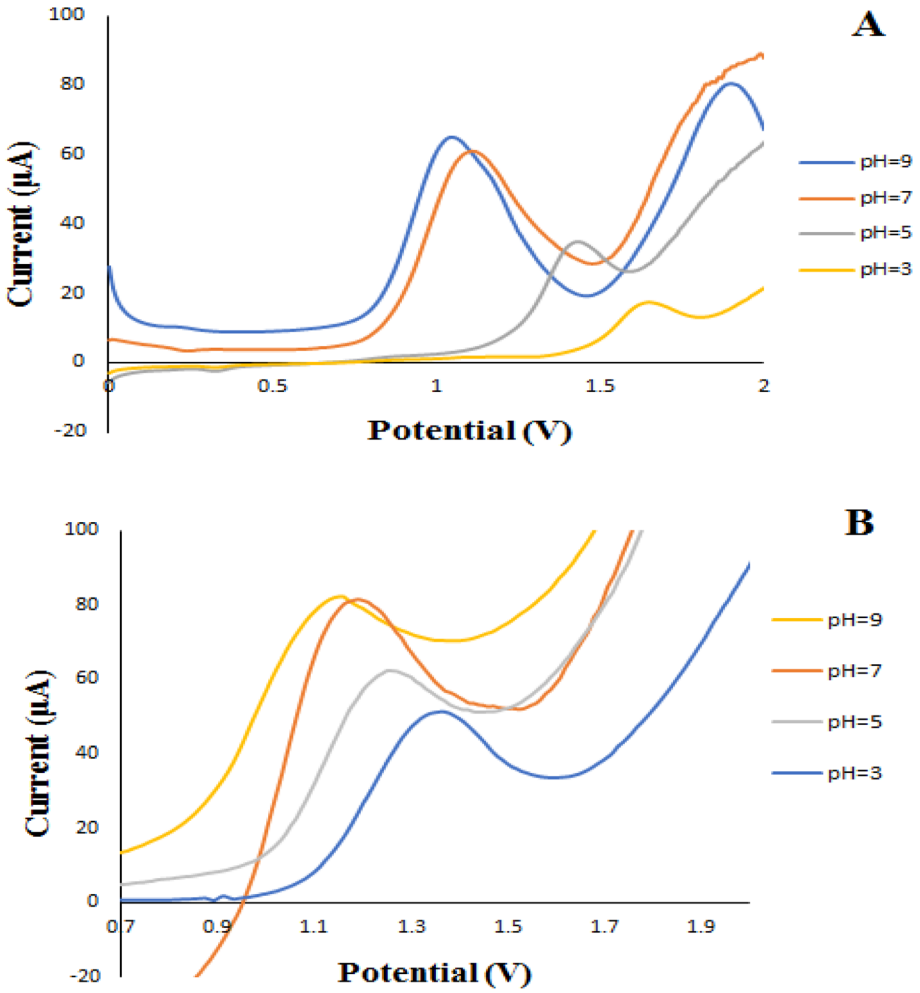

Fig. 3 Illustration of the effect of pH of 300 μg per mL EZP in 0.04 M BR buffer solution on both peak current and peak potential using blank corrected (A) DP-voltammograms obtained by potentiodynamically PPGE, (B) SW-voltammograms obtained by potentiostatically PPGE.

NaCl solution, pH 7, was selected as the optimal pretreatment approach before SWV measurements (Fig. 2B). Under these conditions, the EZP oxidation peak current was enhanced by a factor of 1.30.

3.3. Optimization of experimental conditions

3.3.1. The effect of pH. The influence of pH on the response of the PPGE was examined using a 300 μg per mL EZP solution prepared in 0.04 M BR buffer in the pH range of 3 to 9 adjusted by 2 M NaOH. DPV and SWV measurements were employed following potentiodynamic and potentiostatic pretreatments, respectively. As shown in Fig. 3, there was a noticeable increase in the peak current as the pH increased from 3 to 7. Between pH 6.5 and 7.5, the current remained nearly constant, with only a very slight increase observed at pH 9. However, since EZP was reported to undergo rapid degradation in alkaline media, oxidation under such conditions is not recommended.[50] Based on this investigation, pH 7 was the optimal pH for the current work. It is also noteworthy that the EZP oxidation peak shifted toward more negative potentials with increasing pH.

3.3.2. The effect of supporting electrolyte. The impact of supporting electrolyte was also examined using three different supporting electrolytes: 0.04 M acetate buffer, 0.04 M phosphate buffer, and 0.04 M BR buffer at the optimum pH of 7. The highest EZP peak current with the lowest background signal was observed using a 0.04 M BR buffer in both DPV and SWV measurements conducted following potentiodynamic and potentiostatic pretreatments, respectively (Fig. 4).

3.3.3. The effect of ionic strength of the measuring solution. Although the potentiodynamic and potentiostatic pretreatment strategies enhanced the PGE performance and provided higher DPV and SWV EZP signals, they also resulted in an increase in the background current (Fig. S4, SI File). It was noticed that when the strength of the BR buffer decreased from 0.04 M to 0.01 M in the presence of 0.1 M NaCl to maintain a constant ionic strength, while keeping the pH at the optimal value of 7, the background signals decreased and the DPV and

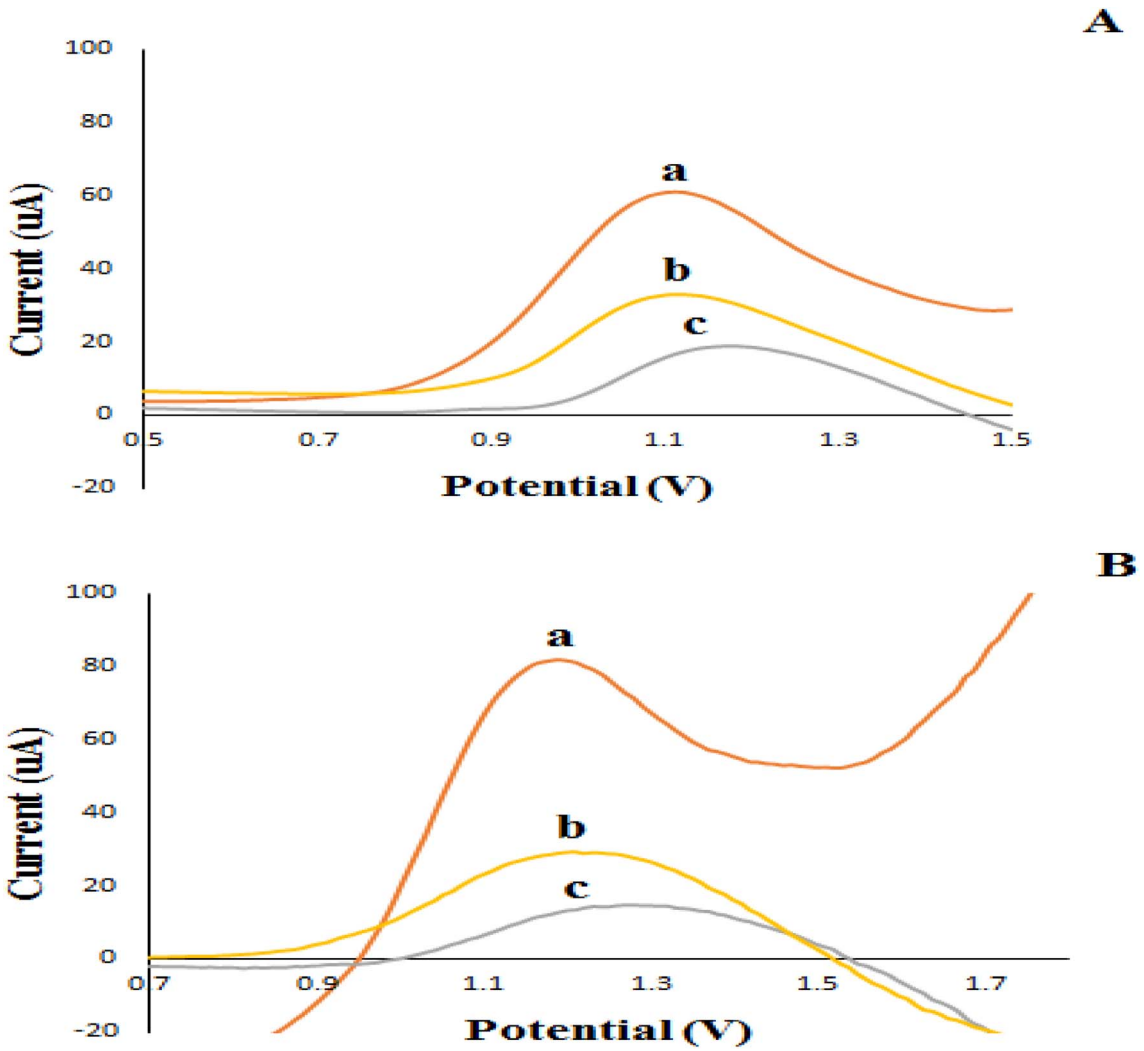

Fig. 4 (A) Blank corrected DP-voltammograms obtained by potentiodynamically PPGE; (B) blank corrected SW-voltammograms obtained by potentiostatically PPGE of 300 μg per mL EZP prepared in (a) 0.04 M BR buffer, pH 7, (b) 0.04 M phosphate buffer, pH 7, and (c) 0.04 M acetate buffer, pH 7.

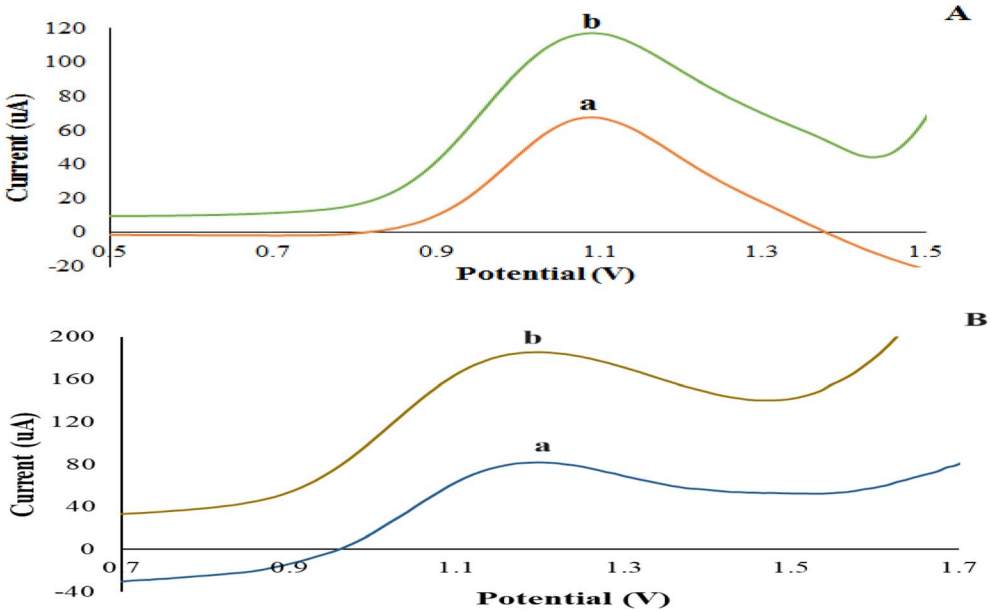

Fig. 5 (A) Blank corrected DP-voltammograms obtained by potentiodynamically PPGE; (B) blank corrected SW-voltammograms obtained by potentiostatically PPGE of (a) 300 μg per mL EZP prepared in 0.04 M BR buffer, pH 7, (b) 300 μg per mL EZP prepared in 0.01 M BR buffer/0.1 M NaCl solution, pH 7.

SWV EZP responses were further increased. Specifically, the EZP peak current was enhanced by approximately a factor of 1.74 and 2.24 for DPV and SWV measurements, respectively (Fig. 5). Consequently, 0.01 M BR buffer/0.1 M NaCl solution, pH 7, was chosen as the optimal measuring solution for further DPV and SWV studies.

3.4. Optimization of DPV and SWV instrumental parameters

The effect of varying the instrumental measurement parameters on the EZP peak current was investigated. For DPV measurements, the influence of pulse time, pulse amplitude, and potential sweep rate on the current intensity of the EZP peak appeared at 1.1009 V was examined. The effect of pulse amplitude on the peak current was investigated within the range of 25–250 mV. A pulse amplitude of 50 mV showed the highest peak current and was therefore selected as the optimal value (Fig. S5A, SI File). Moreover, the pulse time was tested within the range of 0.005–0.1 s. Results showed that, as the pulse time increased, the peak current increased. At higher pulse times, the peak current did not change significantly, and the blank signal showed a very slight increase. Therefore, the optimal pulse time selected was 0.04 s (Fig. S5B, SI File). The effect of varying the scan rate on the peak current was also studied within the range of 20–300 mV s^{-1}. The EZP peak current increased as the scan rates increased; however, higher rates resulted in broader and less defined peaks. Therefore, 80 mV s^{-1} was chosen as the optimal scan rate (Fig. S5C, SI File).

For SWV measurements, the influence of frequency, voltage step, and pulse amplitude on the current intensity of the EZP peak observed at 1.1902 V was examined. The effect of frequency was studied within the range of 20 Hz to 100 Hz. The highest analytical signal, along with a smooth and well-defined peak shape, was observed at 50 Hz (Fig. S6A, SI File). In contrast, peaks recorded at the other frequencies were unsmooth and deformed. Therefore, 50 Hz was chosen as the optimal frequency. The effect of pulse amplitude was evaluated within the range of 10 mV to 100 mV. The EZP signal increased steadily up to 40 mV, beyond which only a slight increase was observed with a significant increase in the blank signal (Fig. S6B, SI File). Consequently, a pulse amplitude of 40 mV was selected as optimal. The effect of the voltage step was investigated within the range of 2 mV to 10 mV. As the voltage step increased, the peak of EZP increased with an insignificant change in the blank signal (Fig. S6C, SI File). Thus, a voltage step of 10 mV was selected as optimal.

3.5. Electrochemical behavior of EZP

To study the electrochemical properties of EZP, CV technique was employed.[51] Fig. 6A represents the cyclic voltammogram of EZP recorded using NPGE, showing a single anodic peak at about 1.3 V with no apparent cathodic peak in the opposite direction. This indicates that the oxidation of EZP is an irreversible electrochemical reaction.

Additionally, CVs of 300 μg per mL EZP prepared in 0.01 M BR buffer/0.1 M NaCl solution, pH 7, were recorded at different scan rates in the range of 0.02–0.3 V s^{-1} (Fig. 6B). As the scan rate (v) increased, a small shift in peak potential (E_p) to the more positive values was observed with a linear increase in the peak current (I_p). This shift in E_p is attributed to the EZP adsorption at the electrode surface as a result of the irreversible electrode process.[52] The inset of Fig. 6B represents the linear relationship between E_p and $\log v$, described by the linear regression equation:

$$E_p\ (\mathrm{V}) = 1.2985 + 0.1204 \log v\ (\mathrm{V\ s^{-1}}),\ r = 0.993$$

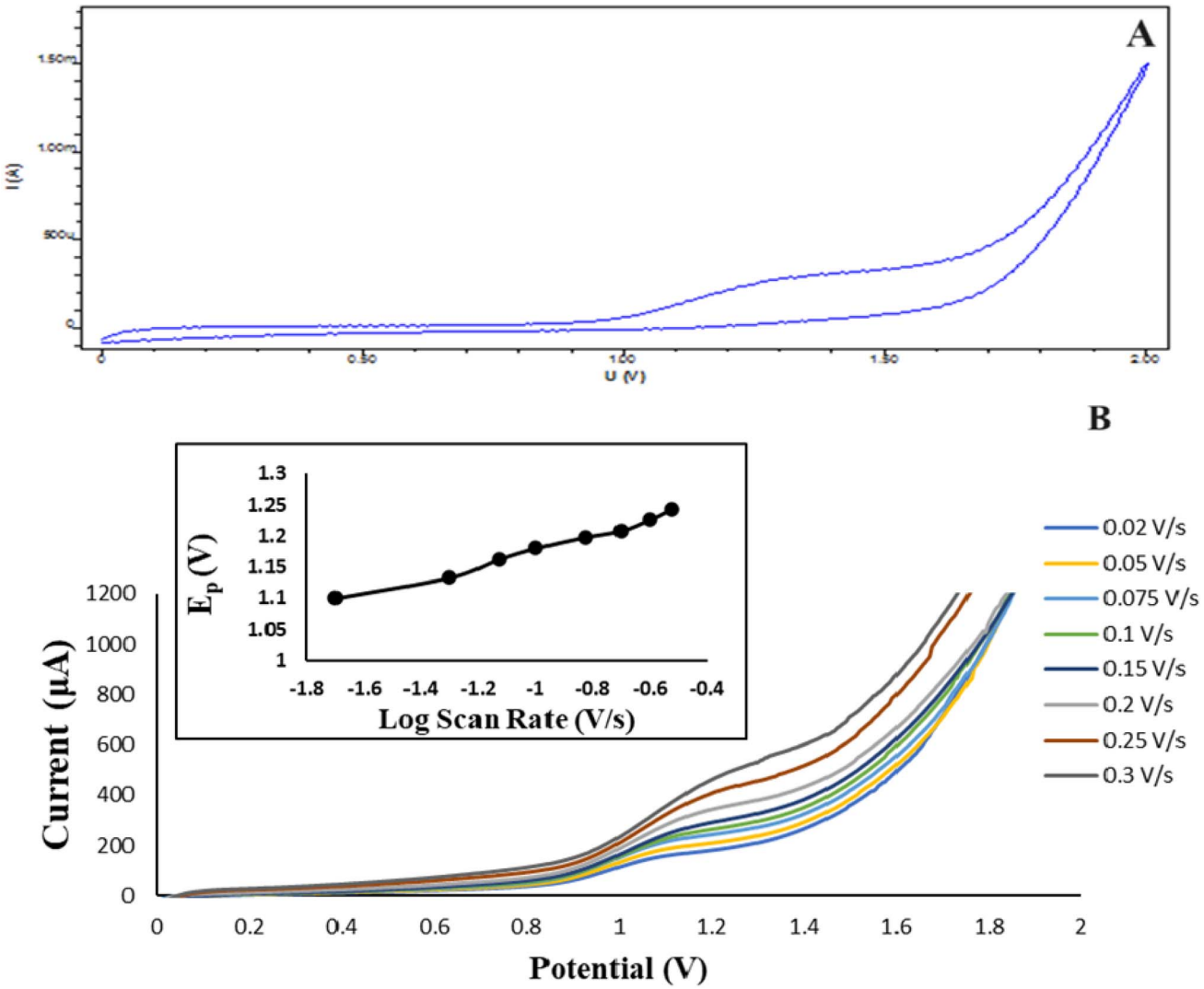

Fig. 6 (A) Cyclic voltammogram of 300 μg per mL EZP in 0.01 M BR buffer/0.1 M NaCl solution, pH 7, using NPGE. (B) Cyclic voltammograms of 300 μg per mL EZP in 0.01 M BR buffer/0.1 M NaCl solution, pH 7, at different scan rates. Inset represents the linear plot between E_p and log scan rate.

The number of electrons transferred for EZP oxidation on the proposed electrode can be calculated based on Laviron's equation for the irreversible systems;[53]

$$E_p(V) = E^0 + \left(\frac{2.303RT}{\alpha nF}\right)\log\left(\frac{RTk^0}{\alpha nF}\right) + \left(\frac{2.303RT}{\alpha nF}\right)\log v$$

where E^0 refers to the formal standard potential; k^0 is the standard heterogeneous reaction rate constant; n is the transfer electron number; α is the charge transfer coefficient. The equation also incorporates fundamental constants: R, the universal gas constant (8.314 J K^{-1} mol^{-1}); T, the absolute temperature (298 K); and F, Faraday's constant (96 485C mol^{-1}).

The (αn) value can be calculated using the slope of E_p and log v plot, which reflects ($2.303RT/\alpha nF$) term in Laviron's equation. Hence the slope is 0.1204; αn is calculated to be 0.491. In case of a totally irreversible electrode process, α is assumed to be 0.5.[54] Consequently, the number of electrons (n) involved in the electrode reaction is 0.982 (≈ 1).

3.6. Proposed EZP oxidation mechanism at PGE

The electrochemical oxidation of EZP at PGE in 0.01 M BR buffer/0.1 M NaCl solution, pH 7 is proposed through an electron transfer mechanism from the tertiary amine moiety of the piperazine ring, which is the most readily oxidized site, generating an unstable radical cation.[55] At neutral pH, the radical cation undergoes rapid deprotonation followed by intramolecular rearrangement to yield a transient iminium ion intermediate. This iminium species is intrinsically unstable in aqueous media and is readily attacked by water, leading to hydrolytic cleavage of the C–N bond. This process results in oxidative *N*-dealkylation, producing the corresponding secondary amine and releasing formaldehyde as the oxidized fragment.

This overall mechanistic pathway is widely recognized for both electrochemical and enzymatic oxidation of tertiary

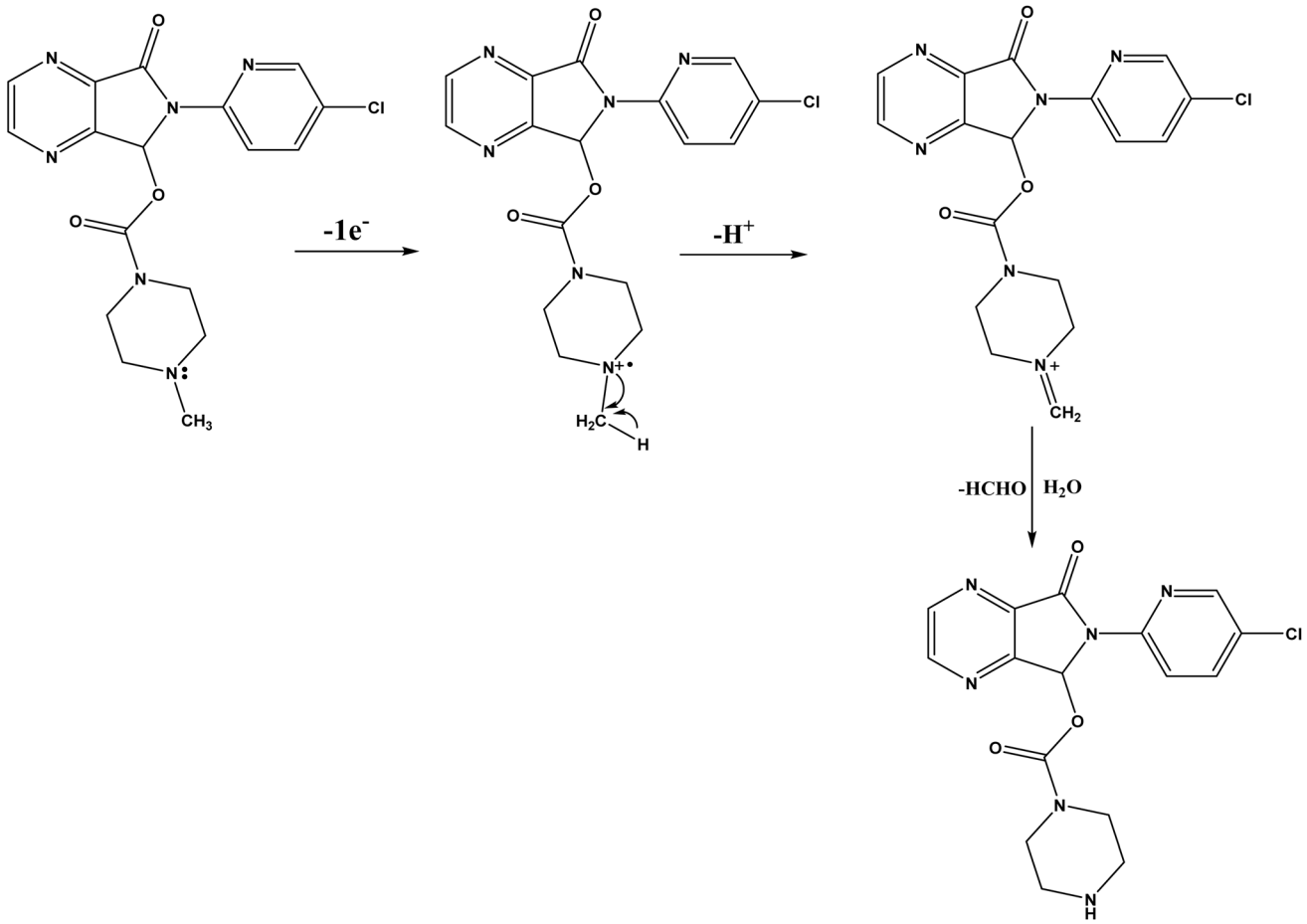

Fig. 7 The proposed EZP Oxidation mechanism at PPGE.

amines, in which an initial one-electron oxidation is followed by iminium ion formation and subsequent hydrolytic *N*-dealkylation. This sequence closely mirrors the oxidative *N*-dealkylation mechanism observed in cytochrome P450 systems.[55,56] The proposed EZP oxidative mechanism is presented in Fig. 7.

3.7. Physiochemical characterization of PGE and PPGE

3.7.1. Fourier transform-infrared (FT-IR) analysis. Both bare PGE and PPGE were characterized using FT-IR to identify the functional groups attached on the electrode surface after the electrochemical pretreatment in 0.04 M BR buffer/0.1 M NaCl solution, pH 7.[57]

Rotring pencil leads utilized in this study consist of carbon, oxygen, and silicon.[58] The FT-IR spectra of PGE and PPGE (Fig. 8) displayed similar bands corresponding to the C=C bond vibrations from graphite, as well as Si–O and Si–O–C bond vibrations from clay minerals present in Rotring pencil leads.[59] The FT-IR spectrum of PGE showed C=C bonds (bending at 665 cm^{-1} and stretching at 1650 cm^{-1}). After the electrochemical pretreatment, these bands shifted to 595 cm^{-1} and 1633 cm^{-1}, respectively. Additionally, the bands of Si–O–Si at 926 cm^{-1},[60] and Si–O–C at 1178 cm^{-1} appeared in the FT-IR spectrum of bare PGE[61] shifted to 848 cm^{-1} and 1068 cm^{-1}, respectively, after pretreatment. Bands of C–H asymmetric/symmetric stretching bonds at 2700–2900 cm^{-1} were observed in both spectra.

The successful oxidative pretreatment of the electrode surface was evidenced by the appearance of a characteristic O–H band at 3441 cm^{-1} only in the PPGE spectrum, indicating the introduction of oxygen containing group to the surface of PGE. This was achieved using a cost-effective and green mild electrolyte and a simple electrochemical pretreatment technique suitable for industrial applications,[62,63] rather than reliance on heating in highly concentrated acids of hazardous and corrosive nature to introduce various oxygen-containing functional groups to the surface of PGE.[64]

The introduction of OH groups and other oxygen-containing functionalities to the surface of PGE through electrochemical treatment is a strategic modification resulting in surface activation that can significantly enhance the electrode's performance. The electrochemical treatment can lead to partial exfoliation of the graphite layers, which increases the surface area available for electrochemical reactions.[33]

Moreover, the introduction of OH groups can create active sites that promote faster electron transfer kinetics, which is beneficial for sensing applications.[33] These functional groups can also contribute to the stability of the electrode response

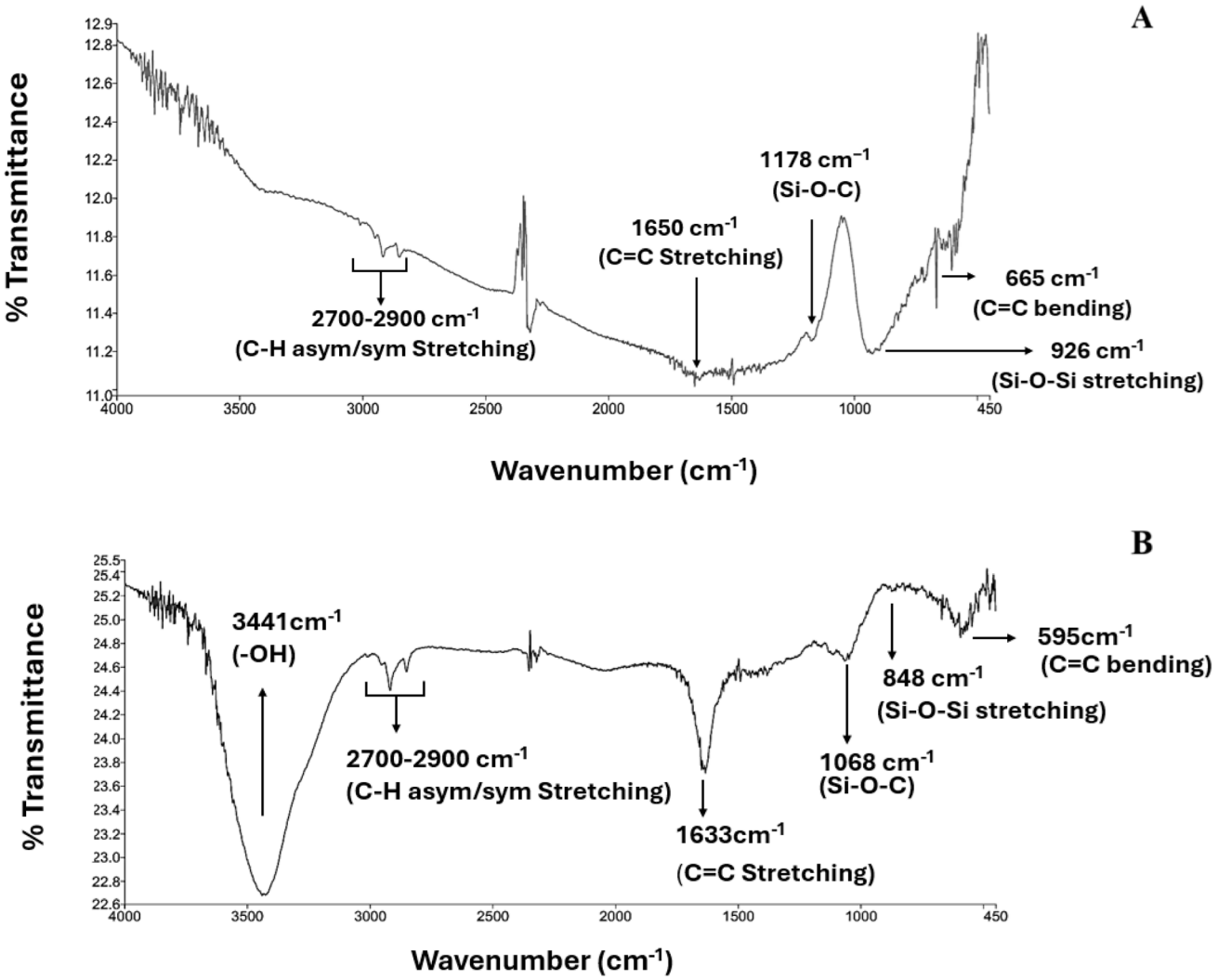

Fig. 8 FT-IR spectra of (A) bare PGE, (B) PPGE.

through stabilization of the reactive intermediates formed during electrochemical reactions, which can improve the overall efficiency of the process, making it more reliable for repeated measurements.[33] Additionally, they increase the hydrophilicity of the electrode surface that can improve the electrode's wettability and its interaction with analytes.[33]

Overall, the electrochemical treatment of PGEs to introduce OH groups is a crucial step in preparing these electrodes for various electroanalytical applications, particularly in biosensing, where sensitivity and selectivity are paramount.

3.7.2. X-ray diffraction (XRD) analysis. The structure of PGE and PPGE was investigated using the XRD technique. The XRD pattern of PPGE (Fig. 9B) showed a sharp diffraction peak at 25.9° with two smaller peaks at 43.6° and 54.1°. These peaks are characteristic of graphitic carbon. When compared to the XRD pattern of PGE (Fig. 9A), no significant differences in the peak positions or broadening were observed.

The similarity in the XRD patterns between PGE and PPGE indicates that the OH functional groups introduced during the electrochemical pretreatment process did not significantly alter the core crystalline structure of the graphite.[65–67] In addition, this suggests that the interlayer spacing between the layers of graphene in the graphite has not changed. This implies that the electrochemical treatment does not cause any expansion or contraction of the crystal lattice.[65–67] Furthermore, the absence of peak broadening suggests that the graphite structure remains well-ordered.[65–67] These provide a positive outcome that the electrochemical treatment is non-destructive, which is beneficial for maintaining the integrity and properties of the electrode material.[62]

3.7.3. Scanning electron microscope (SEM) imaging. The surface morphology of PGE and PPGE was investigated using SEM imaging. The bare PGE exhibits a smooth surface (Fig. 10A–C). After the electrochemical treatment, the surface becomes rough and the graphite particles agglomerate (Fig. 10D–F). The surface morphological changes suggest an increase in the surface area and reaction-active sites.[68,69] This study aligns with the FT-IR and XRD characterization studies confirming that the electrochemical treatment has effectively functionalized the surface of PGE.

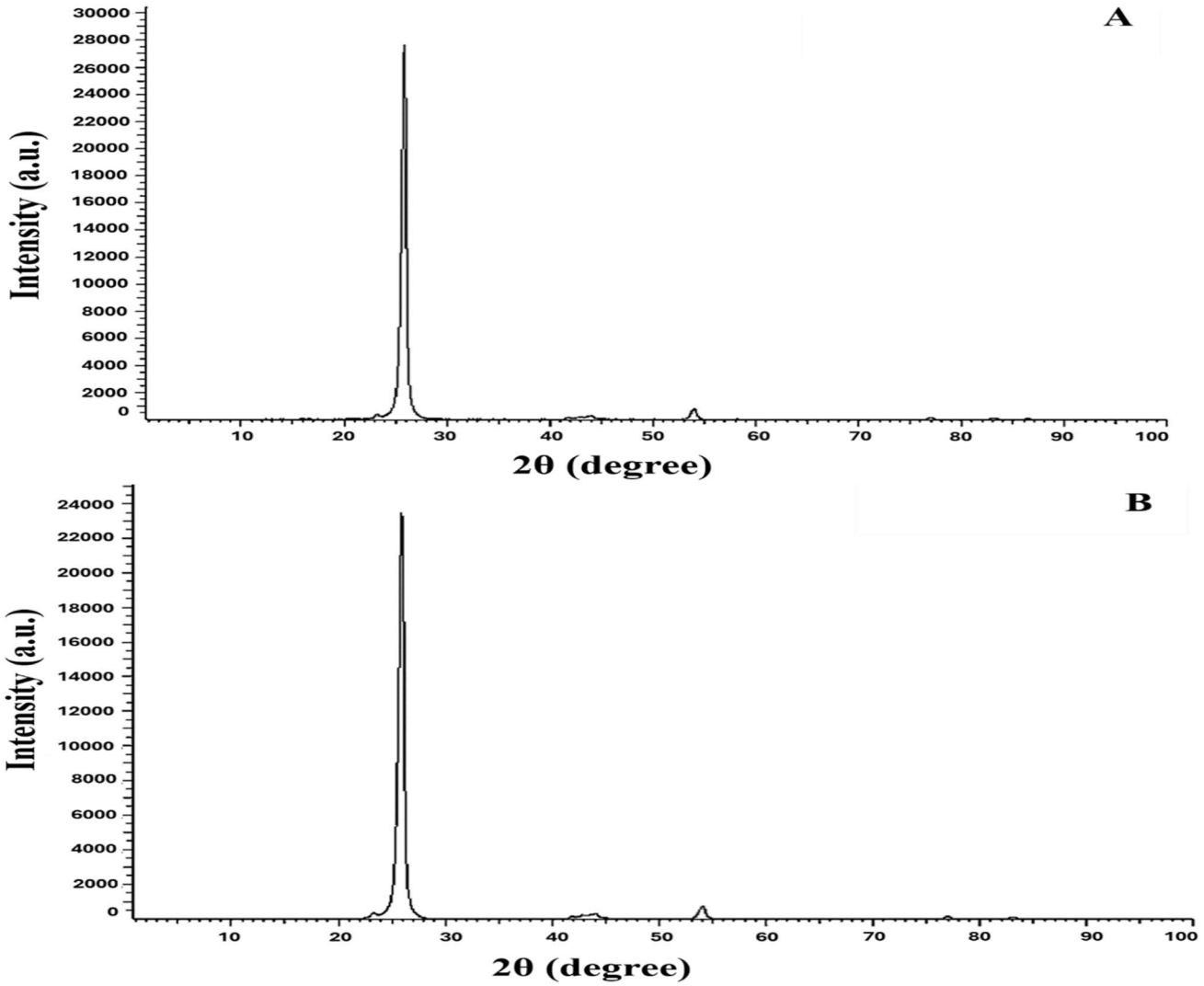

Fig. 9 X-ray diffraction patterns of (A) bare PGE and (B) PPGE.

3.8. Influence of surfactants on the EZP analytical signal

The effect of surfactant addition on the DPV response of EZP was investigated using a potentiodynamically PPGE. Various surfactant types and concentrations, below their critical micelle concentration (CMC), were added to a 300 μg per mL EZP solution prepared in 0.01 M BR buffer, pH 7. The resulting peak currents were compared to that of 300 μg per mL EZP standard solution prepared in 0.01 M BR buffer/0.1 M NaCl solution, pH 7. The results showed that the cationic surfactant CTAB, tested at concentrations of 4×10^{-5} M, 4×10^{-4} M, and 1×10^{-3} M, as well as the non-ionic surfactant tween 80 at concentrations of 5×10^{-7} M, 1×10^{-6} M, and 8×10^{-6} M, did not produce any enhancement in the peak current. In contrast, the anionic surfactant SDS at concentrations of 4×10^{-5} M, 4×10^{-4} M, and 4×10^{-3} M, resulted in an enhancement of the EZP peak current. Among these, 4×10^{-3} M SDS produced the highest peak current and was therefore selected as the optimal concentration (Fig. 11).

The pronounced enhancement in the EZP oxidation current in the presence of SDS can be attributed to the interfacial and electrostatic modifications introduced by the anionic surfactant at the PPGE surface. During the anodic scan, SDS adsorbs onto the positively polarized electrode, generating a negatively charged and more hydrophilic interfacial layer. This surface modification promotes greater EZP preconcentration at the electrode interface through favorable electrostatic interactions and improved wettability.[70–72] Additionally, SDS monomers can orient EZP molecules into more electroactive configurations, inducing specific molecular orientations on the electrode surface that enhance electroactivity and facilitate faster electron-transfer kinetics at the PPGE interface.[72,73] Together, these synergistic effects account for the pronounced increase in oxidation current observed at SDS concentrations below the CMC.

3.9. Influence of adsorptive stripping on the EZP voltammeric analysis

The adsorptive stripping voltammetric (AdSV) approach was applied as an effective preconcentration step prior to the voltammetric measuring of EZP to enhance electroanalytical

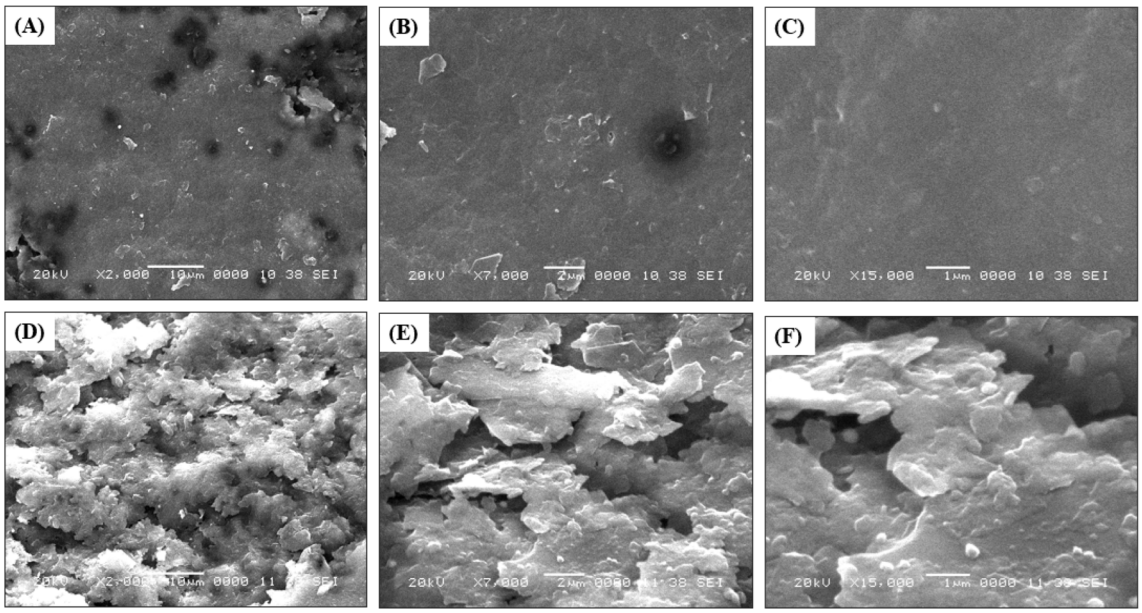

Fig. 10 SEM surface images of bare PGE (A–C) and PPGE (D–E) at resolutions 10 μm (A and D), 2 μm (B and E) and 1 μm (C and F).

sensitivity. This methodology depends on the analyte preconcentration onto or into the working electrode, which is followed by a potential scan that strips the accumulated analyte back into the solution.[74,75]

The optimization of AdSV parameters (accumulation time and potential) was performed using potentiodynamically PPGE, followed by DPV measurement under the optimized conditions, listed in Experimental section 2.3. Regeneration of the electrode was performed after each measurement by immersing it in a blank solution and scanning several cycles till the reading reached the limiting current. The optimized conditions for AdSV were determined to be an accumulation time of 30 s at a preconcentration potential of +0.1 V, as shown in Fig. S7, SI File.

Following the optimization of AdSV conditions, the instrumental parameters for the subsequent DPV measurement were optimized to achieve the maximum peak sensitivity at 1.1009 V. The optimal conditions of DP-AdSV measurements of EZP in 0.01 M BR buffer/0.1 M NaCl solution, pH 7, were found to be the same as the DPV measurements performed without stripping, which were as follows: pulse time = 0.04 s, pulse amplitude = 50 mV, and potential sweep rate = 80 mV s^{-1}.

The high sensitivity achieved by the AdSV technique, as presented in Table 1, can be attributed to the synergistic interplay between the diffusion-controlled accumulation and the adsorption-controlled stripping steps. During the accumulation stage, EZP molecules are transported from the bulk solution to the electrode surface predominantly by diffusion under the applied controlled potential. This process enables continuous preconcentration of EZP at the electrode–solution interface, leading to a significant increase in the local surface concentration relative to the bulk solution. Subsequently, EZP molecules are strongly adsorbed onto the electrode surface, forming a stable adsorbed layer. In the stripping step, the

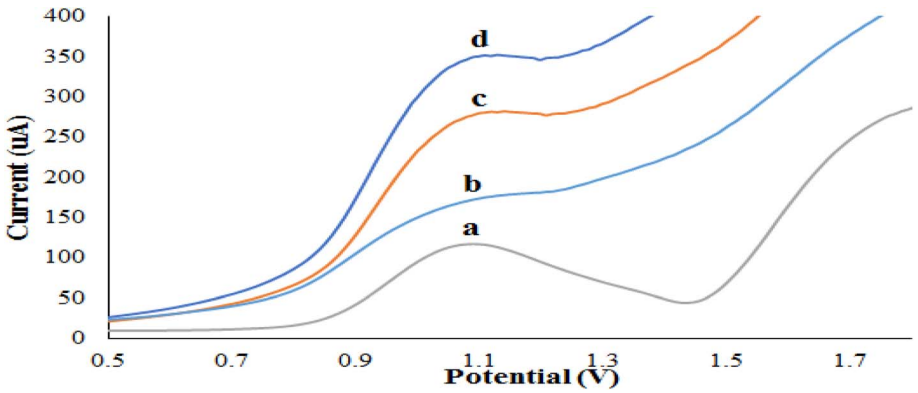

Fig. 11 Blank corrected DP-voltammograms obtained by potentiodynamically PPGE of 300 μg per mL EZP prepared in (a) 0.01 M BR buffer/0.1 M NaCl solution, pH 7, (b) 0.01 M BR buffer/0.00004 M SDS solution, pH 7, (c) 0.01 M BR buffer/0.0004 M SDS solution, pH 7, (d) 0.01 M BR buffer/0.004 M SDS solution, pH 7.

Table 2 Accuracy and precision for the determination of EZP in bulk form using SWV, DPV, and DP-AdSV techniques

Technique	Nominal value (μg mL^{-1})	Within-day			Between-days		
		Found ± SD[a] (μg mL^{-1})	RSD[b] (%)	E_r[c] (%)	Found ± SD[a] (μg mL^{-1})	RSD[b] (%)	E_r[c] (%)
SWV (blank; 0.01 M BR buffer/0.1 M NaCl solution, pH 7)	25	25.47 ± 0.14	0.55	1.88	25.29 ± 0.38	1.52	1.16
	100	100.42 ± 0.93	0.93	0.42	100.21 ± 0.82	0.82	0.21
	300	299.60 ± 0.92	0.31	−0.13	300.55 ± 1.08	0.36	0.18
DPV (blank; 0.01 M BR buffer/0.1 M NaCl solution, pH 7)	25	24.90 ± 0.39	1.57	−0.40	25.27 ± 0.48	1.89	1.08
	100	99.85 ± 0.78	0.78	−0.15	100.34 ± 1.60	1.60	0.34
	300	300.42 ± 0.91	0.30	0.14	299.62 ± 1.67	0.56	−0.13
DPV (blank; 0.01 M BR buffer/0.004 M SDS solution, pH 7)	10	10.17 ± 0.08	0.82	1.70	9.93 ± 0.13	1.31	−0.70
	50	50.89 ± 0.74	1.46	1.78	50.72 ± 0.89	1.75	1.44
	200	200.60 ± 0.83	0.41	0.30	200.75 ± 0.73	0.36	0.38
DP-AdSV (blank; 0.01 M BR buffer/0.1 M NaCl solution, pH 7)	0.25	0.253 ± 0.003	1.27	1.06	0.253 ± 0.004	1.42	1.11
	5	4.97 ± 0.01	0.25	−0.60	4.94 ± 0.04	0.78	−1.20
	15	15.10 ± 0.05	0.30	0.67	15.23 ± 0.06	0.37	1.53

[a] Mean ± standard deviation for three determinations. [b] % Relative standard deviation. [c] % Relative error.

current response depends on the amount of adsorbed species rather than their bulk concentration. As a result, even very low analyte levels produce a measurable signal. This dual mechanism effectively enhances the signal-to-noise ratio, ultimately providing the excellent sensitivity and low detection limits characteristic of AdSV.[76]

3.10. Validation of the voltammetric measurement techniques

The validation of the developed method was performed according to the ICH recommendations.[77]

3.10.1. Linearity ranges and detection/quantitation limits. To validate the current-concentration linear relationship, the calibration plots were constructed under the optimized conditions for DPV, SWV, and DP-AdSV techniques in 0.01 M BR buffer/0.1 M NaCl solution, pH 7, as well as for the DPV technique in 0.01 M BR buffer/0.04 M SDS solution, pH 7 (Fig. S8, SI File). The results revealed a linear relationship between the peak currents and EZP concentrations, with correlation coefficients greater than 0.9999 (Table 1).

The detection limit, $(3s)/m$, and quantitation limit, $(10s)/m$, were calculated, where s is the standard deviation of peak currents for six runs and m is the slope of the calibration curve.[78] The calculated values are presented in Table 1.

3.10.2. Accuracy and precision. The accuracy of the proposed voltammetric techniques was assessed using three different concentrations of standard EZP covering the specified range, each repeated three times (Table 2). In addition, the recovery data calculated from tablet dosage form analysis aided in the further verification of the accuracy of the proposed method (Table 3). The high accuracy of the developed method was indicated by the high recoveries with low percentage errors.

The repeatability (intra-day precision) of the current measurements was evaluated by the triplicate analysis of three different concentrations of EZP within the same day. On the other hand, the reproducibility (inter-day precision) was assessed by the triplicate analysis of the same three concentration levels of EZP on three consecutive days. The relative standard deviations (% RSD) of the peak current values obtained from repeatability and reproducibility studies were calculated and listed in Table 2. All % RSD values were less than 2%, indicating the good precision of the proposed method and their suitability for the routine analysis of EZP in quality control laboratories.

Moreover, electrode-to-electrode reproducibility was evaluated using pencil leads from different manufacturing batches. As shown in Table 4, the low RSD and error values confirm good reproducibility and robustness of the proposed PGE.

Table 3 Determination of EZP in Night Calm® tablets (3 mg per tablet) by the DPV and DP-AdSV techniques

	Proposed DPV method using PPGE	Proposed DP-AdSV method	Reference HPLC method[48]
% recovery (mean ± SD)[a]	(15 μg mL^{-1})	(0.5 μg mL^{-1})	98.01 ± 0.96
	102.51 ± 0.62	96.92 ± 0.77	
	(100 μg mL^{-1})	(5 μg mL^{-1})	
	97.72 ± 0.51	101.85 ± 0.55	
	(300 μg mL^{-1})	(10 μg mL^{-1})	
	98.28 ± 0.79	98.77 ± 0.62	
Student's t-test	0.54	1.63	
Variance ratio F-test	1.46	2.35	

[a] Results of three analysis. Theoretical values for t and F at $P = 0.05$ are 2.23 and 5.05, respectively.

Table 4 Evaluation of electrode-to-electrode reproducibility using different pencil-lead batches at a fixed eszopiclone concentration (100 μg mL^{-1}) by the DPV technique

Electrode batch	Found ± SD [a] (μg mL^{-1})	RSD (%)	E_r (%)
Batch 1	100.25 ± 0.30	0.30	0.25
Batch 2	100.26 ± 0.88	0.88	0.26
Batch 3	99.81 ± 0.95	0.95	−0.19

[a] Mean concentration found ± standard deviation for three determinations ($n = 3$).

3.11. Determination of EZP tablet dosage from

The proposed DPV and DP-AdSV techniques were successfully applied for EZP determination in its tablet formulation, with no sign of interference from the excipients using the optimized measurement conditions. The assay results indicate satisfactory accuracy and precision as reflected by good recovery and RSD values, respectively (Table 3). To further validate the reliability of the developed techniques, statistical comparisons were made with a previously reported HPLC method[48] using a Student's *t*-test and a variance ratio *F*-test. At a 95% confidence level, the experimental *t* and *F* values did not exceed the critical value, as shown in Table 3. These findings indicate good data agreement between the methods and provide additional evidence for the applicability and reliability of the developed voltammetric techniques for routine analysis of EZP in tablet dosage form.

3.12. Determination of EZP in the presence of its alkaline degradants

The applicability of the proposed DPV technique for determining EZP in the presence of its alkaline degradants was evaluated using laboratory-prepared mixtures containing intact EZP and varying proportions of its alkaline degradants (ranging from 1% to 70%). The results, presented in Table S1, SI File, show that the calculated recoveries of EZP at 1.1009 V remained within the range of 98% to 99% for mixtures containing up to 50% degradants. In the presence of 60% degradants, a negligible increase in recovery to 105% was observed. However, when the proportion of degradants reached 70%, slight interference was evident, with the recovery rising to 127%. Fig. S9A, SI File, presents the voltammogram of standard EZP, while Fig. S9B, SI File, shows the voltammogram of EZP in the presence of 70% alkaline degradants.

To verify the source of interference, a solution containing 210 μg mL^{-1} of the degradants, equivalent to 70% of the degradant content in the mixtures, was prepared and analyzed. The resulting DP voltammogram (Fig. S9C, SI File) showed a small peak at 1.0414 V with a current of 28.2 μA after blank correction, confirming the presence of an interfering signal. These findings demonstrate that the proposed method can reliably quantify EZP in the presence of up to 60% of its alkaline degradants, with acceptable accuracy and selectivity.

3.13. Selectivity and interference studies

The selectivity of the proposed PPGE-based voltammetric method was unequivocally demonstrated through its ability to discriminate EZP from both pharmaceutical excipients and structurally related alkaline degradation products. Tablet excipients exhibited no measurable electroactivity within the potential window of interest, and the EZP oxidation peak maintained its characteristic anodic position and shape, confirming the absence of matrix-induced peak distortion or suppression. Furthermore, the method preserved quantitative accuracy in the presence of substantial levels of alkaline degradants, with recoveries consistently ranging between 98–105% for mixtures containing up to 60% degradant content, indicating that the degradants neither overlap with nor significantly influence the EZP oxidation process. Only at extreme degradation levels (70%) did slight interference occur, attributable to the emergence of a minor degradant peak at 1.0414 V, which is adjacent to but still distinct from the EZP peak at 1.1009 V, demonstrating that interference becomes relevant only when degradants vastly exceed the analyte concentration. The ability to resolve EZP in the presence of both inactive excipients and chemically related degradation species underscores the intrinsic specificity of the oxidation process at the PPGE surface. This behavior is supported by the irreversible and adsorption-controlled electron-transfer mechanism of EZP, which favors selective accumulation at the activated PPGE surface, thereby providing inherently high selectivity even in complex matrices. Collectively, these findings confirm the method's strong selectivity and its suitability as a robust stability-indicating tool for routine pharmaceutical quality control.

Additionally, a detailed tolerance study was performed to assess the selectivity of the proposed method for EZP determination. Various inorganic ions and excipients commonly present in pharmaceutical formulations were investigated at interferent-to-EZP concentration ratios of 400 : 1, 600 : 1, 800 : 1, 1000 : 1 and 1200 : 1. The tolerance limit is expressed as the maximum concentration ratio of an interfering species relative to a fixed EZP concentration (10 μg mL^{-1}) that causes a change in the peak current (ΔI_p) not exceeding ±5%.[79] The percentage change in peak current (ΔI_p%) was calculated using the following equation:

$$\Delta I_p(\%) = \frac{I_{p(EZP+interferent)} - I_{p(EZP)}}{I_{p(EZP)}} \times 100$$

where $I_{p(EZP)}$ and $I_{p(EZP+interferent)}$ represent the peak currents of EZP in the absence and presence of the interfering species, respectively.

The tolerance limits obtained for the investigated interferents are summarized in Table 5. Based on the results of the interference study, the proposed method demonstrated sufficient selectivity in the presence of common pharmaceutical excipient.

3.14. Comparison of voltammetric response of EZP using NPGE, PPGE, and GCE

The electrochemical oxidation of EZP at GCE was studied using DPV and SWV techniques in the same buffer solution: 0.01 M BR buffer/0.1 M NaCl solution, pH 7. Before each measurement,

Table 5 Tolerance limit of common inorganic ions and pharmaceutical excipients in the determination of 10 μg mL^{-1} EZP using the proposed PPGE-DPV technique

Interfering species	Tolerance limit ($C_{Interferent} : C_{EZP}$)
Ca^{2+}	400 : 1
K^{+}	600 : 1
Na^{+}	800 : 1
Glucose	800 : 1
Lactose	1000 : 1
Starch	1200 : 1

GCE was manually polished using 0.5 μm alumina dispersed in deionized water, thoroughly rinsed with deionized water, and gently dried using tissue paper.

For DPV measurements at GCE, the DP-voltammogram was recorded from 0 to 2 V against an Ag/AgCl reference electrode using the optimized measuring parameters: pulse time = 0.02 s, pulse amplitude = 200 mV, and potential sweep rate = 80 mV s^{-1}. At a concentration of 300 μg per mL EZP, an anodic DPV peak was observed at 1.0474 V (Fig. 12A). When comparing the voltammetric responses of the same EZP concentration at GCE, NPGE, and PPGE, GCE showed a lower EZP response and a higher background current than PPGE. Specifically, the current response at GCE was 2.51 times lower than that at PPGE. In contrast, GCE showed a slightly higher current response than NPGE by a factor of 1.15, though still accompanied by a higher background current (Fig. 12A).

For SWV measurements at GCE, the following optimum parameters were employed: frequency = 50 Hz, pulse step = 10 mV, and pulse amplitude = 80 mV. A concentration of 300 μg per mL EZP exhibited an anodic SWV peak at 1.1208 V (Fig. 12B). The same concentration was subsequently analyzed using a NPGE and a potentiostatically PPGE, and the results were compared. As shown in Fig. 12B, GCE exhibited a significantly lower current response with a higher background signal compared to both NPGE and PGE. Specifically, the current response at GCE was lower by factors of 1.91 and 2.58 relative to NPGE and PPGE, respectively.

3.15. Assessment of greenness and whiteness of the proposed method

Analytical methodology should be designed to balance the need for environmental sustainability with functional performance, achieving a high level of accuracy and precision while saving time and money and the use of hazardous resources.[80] In line with this, the greenness and whiteness of the proposed method were assessed and compared with previously reported methods for EZP determination. The comparative methods include a spectrophotometric method[5] based on the direct absorbance measurement of the EZP peak at 305 nm, an HPTLC method[16] using silica gel 60F-254 as the stationary phase, methanol–water (6 : 4, v/v) as a mobile phase, and detection at 300 nm, and an

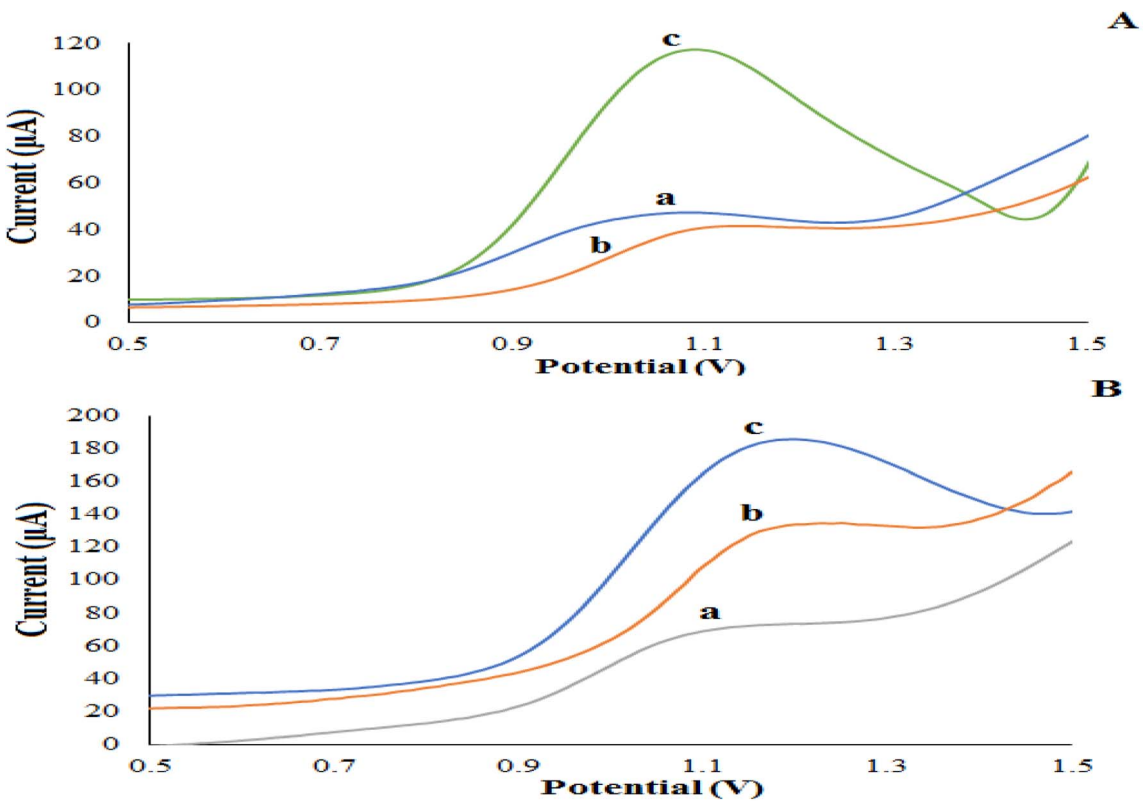

Fig. 12 (A) Blank corrected DP-voltammograms; (B) blank corrected SW-voltammograms of 300 μg per mL EZP in 0.01 M BR buffer/0.1 M NaCl solution, pH 7, obtained by (a) GCE, (b) NPGE, (c) PPGE.

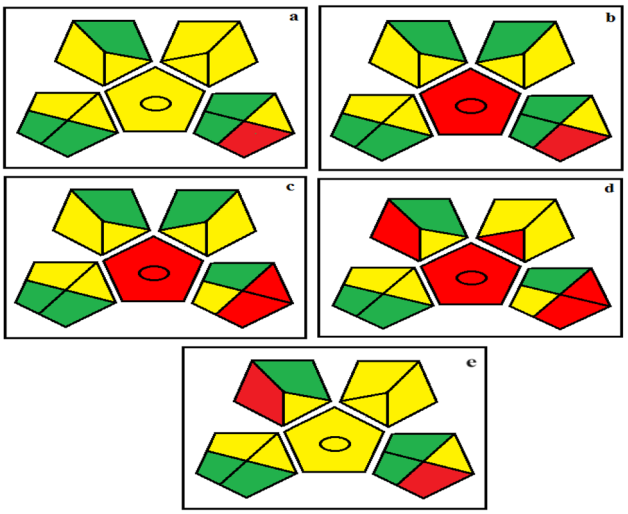

Fig. 13 Greenness assessment using GAPI Pictograms for (a) the proposed PGE method and the previously reported (b) spectrophotometric, (c) HPTLC, (d) HPLC, and (e) DME methods.

HPLC method[12] using a Purospher® Star RP18e column (150 × 4.6 mm; 5μ) in isocratic elution mode. The mobile phase consists of a buffer solution (sodium lauryl sulphate and sodium dihydrogen phosphate monohydrate, pH 3.5) mixed with acetonitrile (50 : 50, v/v), with detection using a photodiode array detector (PDA) at 303 nm. Additionally, the proposed method was compared with a reported voltammetric method[28] that employs DC polarography and AdSV technique on a DME at pH 9 for ZP determination due to the lack of the method's stereo-selectivity. The greenness of the method was assessed based on two modern approaches, namely; Analytical Eco-Scale[81] and GAPI.[82] For whiteness assessment, the multicriteria RGB 12 model approach was applied.[83]

The Analytical Eco-Scale[81] provides information that assesses the greenness of an analytical procedure by evaluating various parameters, including amounts of the solvents and reagents employed, energy consumption, occupational hazards, and the amount of waste generated. Penalty points are given to each parameter, and the final Eco-Scale is calculated by subtracting these penalty points from a total score of 100. As "ideal green analysis" has a value of 100, the closer the Eco-Scale score gets to 100, the more the analytical procedure is green. The developed voltammetric method demonstrated the highest Eco-scale score of 87, compared to other reported methods for EZP determination. Specifically, the spectrophotometric method,[5] HPTLC,[16] and HPLC,[12] scored 85, 82, and 73, respectively (Table S2, SI File). Moreover, the other reported voltammetric method for ZP determination[28] showed a lower score of 79 due to the use of a DME, which poses significant environmental hazards. Consequently, the proposed method has proven to be the most environmentally friendly of all the reported methods.

Compared to the Analytical Eco-Scale, GAPI offers a more detailed and comprehensive assessment of the green character of the whole analytical process, starting from sample collection to final determination.[82] It is based on a color-coded pictogram composed of five pentagrams, each representing a different stage of the analytical workflow. The colors green, yellow, and red are applied to the pentagrams for visual representation of low, moderate, and high environmental impact of each stage, respectively. The listed data in Table S3, SI File, was used to create GAPI pictograms (Fig. 13). Out of all the evaluated methods for EZP analysis, the proposed method demonstrated the lowest environmental impact, as clearly reflected in its GAPI profile.

To assess the overall "whiteness" of the developed method, the multicriteria RGB 12 model[83] was employed. It integrates ecological aspects with functionality. It goes beyond eco-friendliness and safety (represented by green) to also account

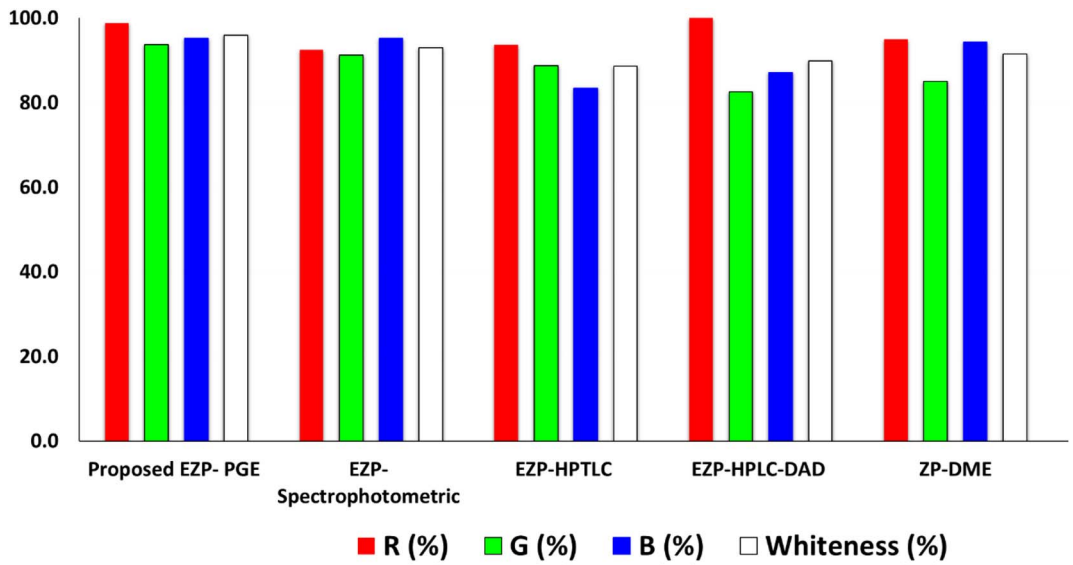

Fig. 14 Comparison of the main evaluation outcomes from RGB 12 analysis for the developed PGE method with other reported methods. The white bar (whiteness %) indicates the arithmetic mean of the three other bars (red, green, and blue).

for analytical performance (red) and practical and economic aspects (blue). Just as the color white results from the combination of red, green, and blue, a method is considered "white" when it successfully meets all three criteria. Using the RGB 12 model, up to 10 analytical methods can be ranked and compared using a single Excel worksheet.[84,85]

The key findings from the whiteness evaluation using the RGB 12 model for the proposed method, in comparison with other reported methods, are presented in Fig. 14 and Table S4, SI File. Both the developed voltammetric method and the reported spectrophotometric method showed the highest score (95.2%) regarding the blue color. This high score is attributed to the use of small reagent volumes, reduced energy consumption, and shorter analysis times. This verifies the high economic impact of these methods over HPLC and HPTLC methods, and even slightly surpass the voltammetric method that uses a DME as a working electrode. Regarding the red criteria, excellent results in all analytical figures of merit, considering the high sensitivity, precision, and accuracy render the developed method possess high analytical performance, with an excellent red score of 98.8%. This high score is justified by the method's broad scope of application; it successfully determined the drug even in the presence of its alkaline degradation products. In terms of detection capability, the proposed method achieved a LOD of 0.058 μg mL^{-1} and a LOQ of 0.195 μg mL^{-1}, which are comparable to or better than those reported for other methods. For instance, the LOD values for the spectrophotometric, HPTLC, and HPLC methods for EZP determination were 0.43 μg mL^{-1}, 0.6 μg mL^{-1}, and 0.054 μg mL^{-1}, respectively, while the voltammetric method for ZP determination showed a LOD of 0.039 μg mL^{-1}. Similarly, the LOQ values for these methods were 0.572 μg mL^{-1}, 0.2 μg mL^{-1}, 0.132 μg mL^{-1}, and 0.389 μg mL^{-1}, respectively.

Regarding the green criteria, the developed PPGE method showed the highest green score of 93.8% due to the usage of smaller volumes of environmentally friendly solvents and reagents, with no energy consumption. By summing up all the above criteria, the developed method shows the highest whiteness percentage of 95.9% compared to the reported methods, Table S4, SI File, which promotes it as a rapid, green, white, and effective method for EZP determination.

3.16. A comparative study with other reported methods

The literature has reported a limited number of analytical methods for the determination of EZP in pharmaceutical dosage forms. The proposed voltammetric method was compared with other reported methods for EZP determination, including a spectrophotometric method reported by Pandya *et al.*,[5] a HPTLC method reported by El-Yazbi *et al.*,[16] and a HPLC method reported by Ravi *et al.*[12] Additionally, it was also compared with a reported voltammetric method developed by Yilmaz[26] for its stereoisomer, ZP, determination. A comparative summary is presented in Table 6, highlighting the analytical performance of the proposed method relative to these reported techniques.[5,12,16,26] The data clearly indicates that our proposed method has the best quantification parameters in terms of the lowest or even comparable LOQ and LOD.

Moreover, a one-way ANOVA statistical test[86] was conducted to compare the recovery data obtained from tablet formulation analysis using the proposed DPV and AdSV methods with those from the reported HPLC method.[48] The results, summarized in Table 7, showed that the experimental *F* value did not exceed the critical value, indicating no significant difference between the methods.

Additionally, our method has been identified as the most eco-friendly, as evaluated by the analytical eco-scale and GAPI approaches. Furthermore, it has been confirmed to have the highest degree of whiteness, as assessed using the RGB 12 model approach. The whiteness of the method reflects a balance between efficacy, functionality, and safety. Thus, the proposed method shown to be an extremely competitive

Table 6 Comparative study between the proposed voltammetric method and other reported methods

Comparison point	EZP proposed DP- AdSV method	EZP reported spectrophotometric method[5]	EZP reported HPTLC method[16]	EZP reported HPLC method[12]	ZP reported DP-AdSV method[26]
Linearity range (μg mL^{-1})	0.25–15	4–24	2–12	49–179	0.23–9.72
LOQ (μg mL^{-1})	0.195	0.572	0.20	0.132	0.205
LOD (μg mL^{-1})	0.058	0.43	0.60	0.054	0.108
Correlation coefficient (*r*)	0.999	0.999	0.996	0.999	0.996

Table 7 Analysis of Variance (ANOVA) of Night Calm® tablets measured by the proposed DPV and AdSV methods and the reported HPLC method.[48]

Source of variation	Sum of squares (SS)	Degree of freedom (df)	Mean squares (MS)	Calculated *F*	Critical *F*
Between groups	1.77	2	0.89	1.38	3.68
Within groups	9.62	15	0.64		
Total	11.39	17			

substitute for the other reported methods, qualifying it for routine quality control applications.

4. Conclusion

The primary goal of the study was to develop a green and efficient method for determining EZP in its pure form, in tablet formulations, and even in the presence of its alkaline degradation products. This was accomplished using various voltammetric techniques (DPV and SWV) with a PPGE as the working electrode. Key factors affecting the EZP signal, including the PGE pretreatment instrumental parameters as well as the electrolyte solution, were carefully optimized. The PPGE-based method proved highly effective, enabling accurate quantification of EZP across a wide concentration range using both DPV and SWV. Compared to traditional GCE, the PPGE significantly enhanced the peak current response and overall sensitivity. Further improvements were achieved by introducing SDS as a surfactant, which not only broadened the detectable concentration range but also lowered the detection and quantification limits. To push sensitivity even further, a DP-AdSV technique was developed. Overall, the study confirms that the proposed method is not only highly sensitive and accurate but also environmentally friendly and well-suited for routine quality control of EZP in pharmaceutical products.

Conflicts of interest

The authors declare that they have no competing interest.

Data availability

All data generated or analyzed during this study are included in this published article and its supplementary information (SI) file. Supplementary information is available. See DOI: https://doi.org/10.1039/d6ra00252h.

References

1 R. E. Franckowski and R. A. Thompson, Eszopiclone (Lunesta™): an analytical profile, *Microgram J.*, 2006, **4**, 29–36.
2 S. C. Sweetman, *Martindale: the Complete Drug Reference*, The Pharmaceutical Press, London, United Kingdom, 36th edn, 2009, p. 995.
3 K. Anandakumar, G. Kumaraswamy, T. Ayyappan, A. S. K. Sankar and D. Nagavalli, Quantitative estimation of eszopiclone in bulk and in formulation by simple UV and difference spectroscopic methods, *Res. J. Pharm. Technol.*, 2010, **3**(1), 202–205.
4 M. Chennaiah, T. Veeraiah and G. Venkateahwarlu, Spectrophotometric determination of eszopiclone in pure and pharmaceutical forms, *J. Chil. Chem. Soc.*, 2012, **57**, 1460–1463, DOI: 10.4067/S0717-97072012000400025.
5 J. Pandya, A. Dubey and P. Prabhu, Development and validation of UV spectrophotometric and RP HPLC method for the estimation of eszopiclone bulk and tablets, *Int. J. Adv. Pharmaceut. Anal.*, 2013, **3**(1), 11–19, DOI: 10.7439/IJAPA.V3I1.38.
6 D. J. Patel, M. J. Patel, J. K. Patel and V. Patel, Simultaneous determination of escitalopram oxalate and eszopiclone in their combined mixture by ultraviolet spectrophotometry (Dual wavelength method), *Anal. Chem.: Indian J.*, 2013, **12**(10), 398–402. https://api.semanticscholar.org/CorpusID:212548789.
7 B. A. Moussa, N. F. Youssef, E. F. Elkady and M. F. Mohamed, Indirect synchronous fluorescence spectroscopy and direct high-performance thin-layer chromatographic methods for enantioseperation of zopiclone and determination of chiral-switching eszopiclone: Evaluation of thermodynamic quantities of chromatographic separation, *Chirality*, 2019, **31**(5), 362–374, DOI: 10.1002/chir.23063.
8 A. Singh and P. Singh, Stability indicating analytical method validation for determination of related substances of eszopiclone in tablet dosage form, *World J. Pharm. Pharmaceut. Sci.*, 2017, **6**(4), 1426–1435, DOI: 10.20959/WJPPS20174-8925.
9 S. Kori, A. Parmar, J. Goyal and S. Sharma, Cloud point extraction coupled with microwave-assisted back-extraction (CPE-MABE) for determination of eszopiclone (Z-drug) using UV–Visible, HPLC and Mass Spectroscopic (MS) techniques: Spiked and in vivo analysis, *J. Chromatogr. B*, 2018, **1074–1075**, 129–138, DOI: 10.1016/j.jchromb.2018.01.005.
10 R. Liu, D. Liu, J. Zhang, H. Zang and Y. Gao, Development of a novel tandem mass spectrometry method for the quantification of eszopiclone without interference from 2-amino-5-chloropyridine and application in a pharmacokinetic study of rat, *J. Pharm. Biomed. Anal.*, 2020, **188**, 113363, DOI: 10.1016/j.jpba.2020.113363.
11 V. Chauhan, M. Sharma, A. Tiwari, V. Tiwari, M. Kumar, A. Sharma, *et al.*, Developing, validating, and comparing an analytical method to simultaneously detect z-drugs in urine samples using the QuEChERS approach with both liquid chromatography and gas chromatography-tandem mass spectrometry, *Saudi Pharm. J.*, 2024, **32**(2), 101950, DOI: 10.1016/j.jsps.2023.101950.
12 D. Ravi, J. V. L. N. Seshagiri-Rao, D. Rajalakshmi and J. Nakka, Development and validation of an RP-HPLC method for the determination of the eszopiclone in tablet dosage forms, *Int. J. Res. Pharm. Chem.*, 2014, **4**, 119–130. https://api.semanticscholar.org/CorpusID:98457360.
13 A. R. P. Lanka, J. V. L. N. S. Rao, P. Srinivasu and P. Vara, UPLC method for the determination of eszopiclone and its related impurities, *Int. J. Anal. Bioanal. Chem.*, 2012, **2**, 241–246, DOI: 10.1093/chromsci/bmt027.
14 N. Sharma, S. Rao, N. Kumar and A. M. Reddy, A novel validated ultra-performance liquid chromatography method for separation of eszopiclone impurities and its degradants in drug products, *J. AOAC Int.*, 2013, **2**(3), 981–986, DOI: 10.5740/JAOACINT.11-489.
15 V. K. Bhusari and S. R. Dhaneshwar, Development and validation of a stability-indicating HPTLC method for the estimation of eszopiclone in pharmaceutical dosage forms,

Asian J. Res. Pharm. Sci., 2021, **11**(3), 219–223, DOI: 10.52711/2231-5659.2021.00035.

16 A. F. El-Yazbi and R. M. Youssef, An eco-friendly HPTLC method for assay of eszopiclone in pharmaceutical preparation: investigation of its water-induced degradation kinetics, *Anal. Methods*, 2015, **7**, 7590–7595, DOI: 10.1039/C5AY01809A.

17 A. F. El-Yazbi and H. M. Ahmed, Green inexpensive capillary electrophoretic method for the determination of Eszopiclone in pharmaceutical preparations, *J. Adv. Pharmaceut. Sci.*, 2024, **1**(1), 1–10, DOI: 10.21608/japs.2024.252648.1006.

18 M. Amare, Voltammetric determination of paracetamol in tablet formulation using Fe (III) doped zeolite-graphite composite modified GCE, *Heliyon*, 2019, **5**, e01663, DOI: 10.1016/j.heliyon.2019.e01663.

19 K. D. Otaif, M. M. Fouad, N. S. Rashed, N. Y. Z. Hosni, A. Elsonbaty and E. Elgazzar, Green prospective approach of chromium zinc oxide nanoparticles for highly ultrasensitive electrochemical detection of anti-hypotensive medication in various matrices, *ACS Omega*, 2023, **8**(33), 30081–30094, DOI: 10.1021/acsomega.3c02381.

20 A. M. Abdel-Raoof, M. M. Fouad, N. S. Rashed, N. Y. Z. Hosni, A. Elsonbaty and A. Abdel-Fattah, Potentiometric determination of mebeverine hydrochloride antispasmodic drug based on molecular docking with different ionophores host–guest inclusion as a theoretical study, *RSC Adv.*, 2023, **13**, 1085–1093, DOI: 10.1039/D2RA06127A.

21 A. M. Abdel-Raoof, A. Elsonbaty, S. Abdulwahab, W. S. Hassan and M. S. Eissa, Potentiometric determination of amprolium drug at a carbon nanotubes/nickel oxide nanoparticles paste electrode, *Microchem. J.*, 2021, **165**, 106185, DOI: 10.1016/j.microc.2021.106185.

22 M. Nejadmansouri, M. Majdinasab, G. S. Nunes and J. L. Marty, An overview of optical and electrochemical sensors and biosensors for analysis of antioxidants in food during the last 5 years, *Sensors*, 2021, **21**(4), 1176, DOI: 10.3390/s21041176.

23 A. F. El-Yazbi, S. M. Sabry, M. S. Moneeb, F. A. H. Elgammal and H. M. Essam, Economic electrochemical sensors for the determination of eszopiclone in pharmaceutical formulation with greenness profile assessment, *Electroanalysis*, 2022, **34**, 1–15, DOI: 10.1002/elan.202200082.

24 A. F. Alghamdi, Validation and application of the square wave voltammetry method for the electrochemical determination of eszopiclone in pharmaceutical formulations and human biological fluids using glassy carbon electrode, *J. King Saud Univ. Sci.*, 2024, **36**(9), 103408, DOI: 10.1016/j.jksus.2024.103408.

25 C. Kaya, K. Birgül and B. Bülbül, Fundamentals of chirality, resolution, and enantiopure molecule synthesis methods, *Chirality*, 2023, **35**(1), 4–28, DOI: 10.1002/chir.23512.

26 S. Yilmaz, Adsorptive stripping voltammetric determination of zopiclone in tablet dosage forms and human urine, *Colloids Surf., B*, 2009, **71**, 79–83, DOI: 10.1016/j.colsurfb.2009.01.007.

27 J. Taborsky, M. Svidrnoch, O. Kurka, L. Borovcova, P. Bednar, P. Bartak, *et al.*, Electrochemical oxidation of zopiclone, *Monatsh. Chem.*, 2016, **147**, 53–60, DOI: 10.1007/s00706-015-1602-9.

28 J. C. Viré, H. Zhang, G. Quarin, G. J. Patriarche, Z. Sentürk and G. D. Christian, Electrochemical behavior of zopiclone, *Talanta*, 1993, **40**(3), 313–323, DOI: 10.1016/0039-9140%2893%2980240-R.

29 Annu, S. Sharma, R. Jain and A. N. Raja, Review—pencil graphite electrode: an emerging sensing material, *J. Electrochem. Soc.*, 2020, **167**, 037501, DOI: 10.1149/2.0012003JES.

30 A. Kosenko, K. Pushnitsa, A. A. Pavlovskii, P. Novikov and A. A. Popovich, The review of existing strategies of end-of-life graphite anode processing using 3Rs approach: recovery, recycle, reuse, *Batteries*, 2023, **9**(12), 579, DOI: 10.3390/batteries9120579.

31 I. G. David, D. Popa and M. Buleandra, Pencil graphite electrodes: A versatile tool in electroanalysis, *J. Anal. Methods Chem.*, 2017, **2017**, 1905968, DOI: 10.1155/2017/1905968.

32 D. G. Dilgin and S. Karakaya, Differential pulse voltammetric determination of acyclovir in pharmaceutical preparations using a pencil graphite electrode, *Mater. Sci. Eng., C*, 2016, **63**, 570–576, DOI: 10.1016/j.msec.2016.02.079.

33 S. Srinivas and A. S. Kumar, Surface-activated pencil graphite electrode for dopamine sensor applications: A critical review, *Biosensors*, 2023, **13**(3), 353. https://www.mdpi.com/2079-6374/13/3/353.

34 R. Rejithamol, R. G. Krishnan and S. Beena, Disposable pencil graphite electrode decorated with a thin film of electro-polymerized 2, 3, 4, 6, 7, 8, 9, 10-octahydropyrimido [1, 2-a] azepine for simultaneous voltammetric analysis of dopamine, serotonin and tryptophan, *Mater. Chem. Phys.*, 2021, **258**, 123857, DOI: 10.1016/j.matchemphys.2020.123857.

35 A. Wong, A. M. Santos, R. da Fonseca-Alves, F. C. Vicentini, O. Fatibello-Filho and M. D. P. T. Sotomayor, Simultaneous determination of direct yellow 50, tryptophan, carbendazim, and caffeine in environmental and biological fluid samples using graphite pencil electrode modified with palladium nanoparticles, *Talanta*, 2022, **222**, 121539, DOI: 10.1016/j.talanta.2020.121539.

36 A. Dehnavi and A. Soleymanpour, Highly sensitive voltammetric electrode for the trace measurement of methyldopa based on a pencil graphite modified with phosphomolibdate/graphene oxide, *Microchem. J.*, 2020, **157**, 104969, DOI: 10.1016/j.microc.2020.104969.

37 E. Alipour, M. R. Majidi, A. Saadatirad, S. M. Golabi and A. M. Alizadeh, Simultaneous determination of dopamine and uric acid in biological samples on the pretreated pencil graphite electrode, *Electrochim. Acta*, 2013, **91**, 36–42, DOI: 10.1016/J.ELECTACTA.2012.12.079.

38 E. Alipour and S. Gasemlou, Easy modification of pencil graphite electrode for discrimination and determination of morphine in biological and street samples, *Anal. Methods*, 2012, **4**, 2962–2969, DOI: 10.1039/C2AY25455G.

39 M. R. Akanda, M. Sohail, M. A. Aziz and A. N. Kawde, Recent advances in nanomaterial-modified pencil graphite electrodes for electroanalysis, *Electroanalysis*, 2016, **28**(3), 408–424, DOI: 10.1002/elan.201500374.

40 M. A. Aziz and A. N. Kawde, Gold nanoparticle-modified graphite pencil electrode for the high-sensitivity detection of hydrazine, *Talanta*, 2013, **115**, 214–221, DOI: 10.1016/j.talanta.2013.04.038.

41 O. Koyun and Y. Sahin, Poly(L-cysteine) modified pencil graphite electrode for determination of sunset yellow in food and beverage samples by differential pulse voltammetry, *Int. J. Electrochem. Sci.*, 2018, **13**, 159–174, DOI: 10.20964/2018.01.40.

42 G. P. Fard, E. Alipour and R. E. A. Sabzi, Modification of a disposable pencil graphite electrode with multiwalled carbon nanotubes: Application to electrochemical determination of diclofenac sodium in some pharmaceutical and biological samples, *Anal. Methods*, 2016, **8**(19), 3966–3974, DOI: 10.1039/C6AY00441E.

43 M. Goudarzi, M. Salavati-Niasari, M. Bazarganipour and M. Motaghedifard, Sonochemical synthesis of Tl_2O_3 nanostructures: Supported on multi-walled carbon nanotube modified electrode for monitoring of copper ions, *J. Mater. Sci.: Mater. Electron.*, 2016, **27**(4), 3675–3682, DOI: 10.1007/s10854-015-4207-5.

44 E. Alipour, M. R. Majidi and O. Hoseindokht, Development of simple electrochemical sensor for selective determination of methadone in biological samples using multi-walled carbonanotubes modified pencil graphite electrode, *J. Chin. Chem. Soc.*, 2015, **62**(5), 461–468, DOI: 10.1002/jccs.201400391.

45 K. Karaboduk, Development of a voltammetric method for the determination of rapamycin in pharmaceutical samples at pretreated pencil graphite electrode, *J. Chin. Chem. Soc.*, 2021, **68**, 1722–1730, DOI: 10.1002/jccs.202100079.

46 A. Ozcan, Synergistic effect of lithium perchlorate and sodium hydroxide in the preparation of electrochemically treated pencil graphite electrodes for selective and sensitive bisphenol a detection in water samples, *Electroanalysis*, 2014, **26**(7), 1631–1639, DOI: 10.1002/elan.201400082.

47 J. Wang, *Stripping Analysis. Deerfield Beach*, VCH Publishers, Inc, Florida, 1985, p. 59.

48 S. R. Dhaneshwar and V. K. Bhusari, Development of a validated stability-indicating HPLC assay method for eszopiclone, *Int. J. ChemTech Res.*, 2011, **2**(2), 680–689.

49 R. C. Engstrom, Electrochemical pretreatment of glassy carbon electrodes, *Anal. Chem.*, 1982, **55**(13), 2310–2314, DOI: 10.1021/ac00250a038.

50 C. Fernandez, F. Gimenez, J. Mayrargue, A. Thuillier and R. Farinotti, Degradation and racemization of zopiclone enantiomers in plasma and partially aqueous solutions, *Chirality*, 1995, **7**(4), 267–271, DOI: 10.1002/CHIR.530070413.

51 C. M. A. Brett and A. M. O. Brett, *Electrochemistry: Principles, Methods, and Applications*, Oxford University Press, Oxford, New York, 1993.

52 H. T. Purushothama, Y. Arthoba-Nayaka, M. M. Vinay, P. Manjunatha, R. O. Yathisha and K. V. Basavarajapp, Pencil graphite electrode as an electrochemical sensor for the voltammetric determination of chlorpromazine, *J. Sci. Adv. Mater. Devices*, 2018, **3**(2), 161–166, DOI: 10.1016/j.jsamd.2018.03.007.

53 E. Laviron, General expression of the linear potential sweep voltammogram in the case of diffusionless electrochemical systems, *J. Electroanal. Chem. Interfacial Electrochem.*, 1979, **101**(1), 19–28, DOI: 10.1016/S0022-0728(80)80496-7.

54 S. K. Lovrić and M. Lovrić, Theory of kinetically controlled electrode reaction coupled to ion transfer across the liquid/liquid interface, *Cent. Eur. J. Chem.*, 2005, **3**(2), 216–229, DOI: 10.2478/BF02475992.

55 D. Bhat and N. Sharma, Oxidative N-dealkylation of tertiary amines with tetraethylammonium periodate catalyzed by metal complexes, *Aust. J. Chem.*, 2016, **70**(3), 233–236, DOI: 10.1071/CH16200.

56 F. P. Guengerich and T. L. Macdonald, Chemical mechanisms of catalysis by cytochromes P-450: a unified view, *Acc. Chem. Res.*, 1984, **17**(1), 9–16, DOI: 10.1021/ar00097a002.

57 D. W. Lee, S. V. L. De-Los, J. W. Seo, L. L. Felix, D. A. Bustamante, J. M. Cole, *et al.*, The structure of graphite oxide: investi gation of its surface chemical groups, *J. Phys. Chem. B*, 2010, **114**(17), 5723–5728, DOI: 10.1021/jp1002275.

58 R. Navratil, A. Kotzianova, V. Halouzka, T. Opletal, I. Triskova, L. Trnkova, *et al.*, Polymer lead pencil graphite as electrode material: Voltammetric, XPS and Raman study, *J. Electroanal. Chem.*, 2016, **783**, 152–160, DOI: 10.1016/j.jelechem.2016.11.030.

59 J. Jaimanee, P. Chatchawal, M. Wongwattanakul, S. Phantanawiboon, C. Leelayuwat and A. Jumnainsong, Application of attenuated total reflectance Fourier-transform infrared spectroscopy in human sera: Validate the method for contributing effective strategy for the storage and preservation, *Vib. Spectrosc.*, 2024, **35**, 103741, DOI: 10.1016/j.vibspec.2024.103741.

60 L. Song, J. Chen, Y. Bian, L. Zhu, Y. Zhou, Y. Xiang, *et al.*, Synthesis, characterization and desulfurization performance of MCM-41 functionalized with cu by direct synthesis and organosilanes by grafting, *J. Porous Mater.*, 2015, **22**(2), 379–385, DOI: 10.1007/s10934-014-9906-4.

61 D. E. Leyden and J. B. Atwater, Hydrolysis and condensation of alkoxysilanes investigated by internal reflection FTIR spectroscopy, *J. Adhes. Sci. Technol.*, 1991, **5**(10), 815–829, DOI: 10.1163/156856191X00233.

62 A. A. AbdelHamid, A. Elgamouza and A. Kawde, Controlled electrochemical surface exfoliation of graphite pencil electrodes for high-performance supercapacitors, *RSC Adv.*, 2023, **13**, 21300, DOI: 10.1039/D3RA03952H.

63 S. Nagarajan, R. Vairamuthu, R. Angamuthu and G. Venkatachalam, Electrochemical fabrication of reusable

pencil graphite electrodes for highly sensitive, selective and simultaneous determination of hydroquinone and catechol, *J. Electroanal. Chem.*, 2019, **846**, 113156, DOI: 10.1016/j.jelechem.2019.05.038.

64 E. Keskin and A. S. Ertürk, Electrochemical determination of paracetamol in pharmaceutical tablet by a novel oxidative pretreated pencil graphite electrode, *Ionics*, 2018, **24**, 4043–4054, DOI: 10.1007/s11581-018-2532-4.

65 S. Hou, J. Li, X. Huang, X. Wang, L. Ma, W. Shen, *et al.*, Silver nanoparticles-loaded exfoliated graphite and its anti-bacterial performance, *Appl. Sci.*, 2017, **7**, 852, DOI: 10.3390/app7080852.

66 J. Lin, Y. Huang, S. Wang and G. Chen, Microwave-assisted rapid exfoliation of graphite into graphene by using ammonium bicarbonate as the intercalation agent, *Ind. Eng. Chem. Res.*, 2017, **56**, 9341–9346, DOI: 10.1021/acs.iecr.7b01302.

67 B. Zhao, L. Jiang, X. Zeng, K. Zhang, M. M. F. Yuen, J. B. Xu, *et al.*, A highly thermally conductive electrode for lithium ion batteries, *J. Mater. Chem. A*, 2016, **4**, 14595–14604, DOI: 10.1039/C6TA04774B.

68 V. N. Ataide, W. A. Ameku, R. P. Bacil, L. Angnes, W. R. Araujo and T. R. L. C. Paixão, Enhanced performance of pencil-drawn paper-based electrodes by laser-scribing treatment, *RSC Adv.*, 2021, **11**, 1644–1653, DOI: 10.1039/D0RA08874A.

69 E. Bernalte, C. W. Foster, D. A. C. Brownson, M. Mosna, G. C. Smith and C. E. Banks, Pencil it in: Exploring the feasibility of hand-drawn pencil electrodes for electrochemical sensing platforms, *Biosensors*, 2016, **6**(3), 45, DOI: 10.3390/bios6030045.

70 J. Kozak, K. Tyszczuk-Rotko, K. Sztanke and M. Sztanke, Sensitive and selective voltammetric sensor based on anionic surfactant-modified screen-printed carbon for the quantitative analysis of an anticancer active fused azaisocytosine-containing congener, *Int. J. Mol. Sci.*, 2023, **24**(1), 564, DOI: 10.3390/ijms24010564.

71 V. B. Patil, D. Ilager, S. M. Tuwar, K. Mondal and N. P. Shetti, Nanostructured ZnO-based electrochemical sensor with anionic surfactant for the electroanalysis of trimethoprim, *Bioengineering*, 2022, **9**(10), 521, DOI: 10.3390/bioengineering9100521.

72 E. K. Savan and D. Kazıcı, Electrochemical applications of surfactants Essential, *Chem*, 2024, **1**(1), 1–10, DOI: 10.1080/28378083.2024.2386523.

73 C. E. Sener, B. D. Topal and S. A. Ozkan, Effect of monomer structure of anionic surfactant on voltammetric signals of an anticancer drug: rapid, simple, and sensitive electroanalysis of nilotinib in biological samples, *Anal. Bioanal. Chem.*, 2020, **412**, 8073–8081, DOI: 10.1007/s00216-020-02934-9.

74 G. M. Swain, Arrigan DWM (Ed.). Electrochemical strategies in detection science, *Anal. Bioanal. Chem.*, 2006, **408**(23), 6245–6246, DOI: 10.1007/s00216-016-9688-4.

75 *Electroanalytical Methods: Guide to Experiments and Applications*, ed. F. Scholz, Springer, 2006, pp. 201–218.

76 M. Adamczyk, M. Grabarczyk and E. Wlazłowska, Fast and simple differential pulse adsorptive stripping voltammetric determination of Ce(III) in natural water samples, *Desalination Water Treat.*, 2022, **264**, 188–195, DOI: 10.5004/dwt.2022.28585.

77 International Conference on Harmonisation of Technical Requirements for Registration of Pharmaceuticals for Human Use, ICH Harmonised Tripartite Guideline, Topic Q2 (R1): Validation of Analytical Procedures: Text and Methodology, Geneva, 2005.

78 S. Skrzypek, W. Ciesielski, A. Sokolowski, S. Yilmaz and D. Kazmierczak, Square wave adsorptive stripping voltammetric determination of famotidine in urine, *Talanta*, 2005, **66**, 1146–1151, DOI: 10.1016/j.talanta.2005.01.017.

79 A. H. Kamel, A. E. Amr and M. A. Al-Omar, Pre-concentration based on cloud point extraction for ultra-trace monitoring of lead (II) using flame atomic absorption spectrometry, *Appl. Sci.*, 2019, **9**(22), 4752, DOI: 10.3390/app9224752.

80 A. Gałuszka, Z. Migaszewski and J. Namieśnik, The 12 principles of green analytical chemistry and the SIGNIFICANCE mnemonic of green analytical practices, *Trends Anal. Chem.*, 2013, **50**, 78–84, DOI: 10.1016/j.trac.2013.04.010.

81 A. Gałuszka, Z. M. Migaszewski, P. Konieczka and J. Namieśnik, Analytical EcoScale for assessing the greenness of analytical procedures, *Trends Anal. Chem.*, 2012, **37**, 61–72, DOI: 10.1016/j.trac.2012.03.013.

82 J. Płotka-Wasylka, A new tool for the evaluation of the analytical procedure: Green Analytical Procedure Index, *Talanta*, 2018, **181**, 204–209, DOI: 10.1016/j.talanta.2018.01.013.

83 P. M. Nowak, R. Wietecha-Posłuszny and J. Pawliszyn, White analytical chemistry: an approach to reconcile the principles of green analytical chemistry and functionality, *Trends Anal. Chem.*, 2021, **138**, 116223, DOI: 10.1016/j.trac.2021.116223.

84 A. R. Ahmed, S. M. Galal, M. A. Korany and M. A. A. Ragab, Multicomponent antihypertensive pharmaceuticals determination with related impurity analysis using MEKC: Whiteness and greenness assessment, *Sustain. Chem. Pharm.*, 2023, **33**, 101066, DOI: 10.1016/j.scp.2023.101066.

85 A. R. Ahmed, M. A. Korany, S. M. Galal and M. A. A. Ragab, Green and white MEKC for determination of different anti-diabetic binary mixtures and their triple-combo pill, *BMC Chem.*, 2023, **17**(1), 86, DOI: 10.1186/s13065-023-00997-0.

86 J. N. Miller and J. C. Miller, *Statistics and Chemometrics for Analytical Chemistry*, Pearson Education Limited, England, 6th edn, 2010, pp. 39–40, 7, 141-2.